Causes of hOCT1-dependent cholangiocarcinoma resistance to sorafenib and sensitization by tumor-selective gene therapy

Journal:	*Hepatology*
Manuscript ID	HEP-18-1287.R2
Wiley - Manuscript type:	Original
Date Submitted by the Author:	n/a
Complete List of Authors:	Lozano, Elisa; University of Salamanca, Laboratory of Experimental Hepatology and Drug Targeting (HEVEFARM) Macias, Rocio; Universidad de Salamanca, Physiology and Pharmacology Monte, Maria; University of Salamanca, Laboratory of Experimental Hepatology and Drug Targeting (HEVEFARM) CIBERehd Asensio, Maitane; Universidad de Salamanca, Physiology and Pharmacology Del Carmen, Sofia; Salamanca University Hospital, IBSAL Sanchez-Vicente, Laura; Universidad de Salamanca, Physiology and Pharmacology Alonso-Peña, Marta; Universidad de Salamanca, Physiology and Pharmacology Al-Abdulla, Ruba; Universidad de Salamanca, Physiology and Pharmacology Munoz-Garrido, Patricia; University of Copenhagen Biotech Research and Innovation Centre, ; Biodonostia Health Research Institute – Donostia University Hospital, Department of Liver and Gastrointestinal Diseases; National Institute for the Study of Liver and Gastrointestinal Diseases (CIBERehd, Instituto de Salud Carlos III) Satriano, Letizia O'Rourke, Colm; University of Copenhagen Biotech Research and Innovation Centre, Health and Medical Sciences Banales, Jesus; Biodonostia Research Institute (Donostia University Hospital), IKEBASQUE (Basque Foundation for Science), University of Basque Country (UPV), San Sebastián, Spain., Department of Liver Diseases Avila, Matias; CIMA. Universidad de Navarra, Division of Hepatology and Gene Therapy Martinez Chantar, Maria; CIC bioGUNE, Metabolomics Andersen, Jesper; University of Copenhagen Biotech Research and Innovation Centre, Health and Medical Sciences Briz, Oscar; University of Salamanca, Laboratory of Experimental Hepatology and Drug Targeting (HEVEFARM) Marin, Jose; Salamanca, Spain, Physiology and Pharmacology
Keywords:	Biliary Tumors, Drug Transport, Chemotherapy, Chemoresistance, Tyrosine Kinase Inhibitors

Causes of hOCT1-dependent cholangiocarcinoma resistance to sorafenib and sensitization by tumor-selective gene therapy

Elisa Lozano[1,7], Rocio I.R. Macias[1,7], Maria J. Monte[1,7], Maitane Asensio[1], Sofia del Carmen[2], Laura Sanchez-Vicente[1], Marta Alonso-Peña[1], Ruba Al-Abdulla[1], Patricia Munoz-Garrido[3], Letizia Satriano[3], Colm J. O'Rourke[3], Jesus M. Banales[4,7], Matias A. Avila[5,7], Maria L. Martinez-Chantar[6,7], Jesper B. Andersen[3], Oscar Briz[1,7], Jose J.G. Marin[1,7]

[(1)] *Experimental Hepatology and Drug Targeting (HEVEFARM), IBSAL, University of Salamanca, Salamanca, Spain.*

[(2)] *Salamanca University Hospital, IBSAL, University of Salamanca, Salamanca, Spain.*

[(3)] *Biotech Research and Innovation Centre, Department of Health and Medical Sciences, University of Copenhagen, Copenhagen, Denmark.*

[(4)] *Department of Hepatology and Gastroenterology. Biodonostia Health Research Institute. Donostia University Hospital. University of the Basque Country (UPV/EHU). Ikerbasque. San Sebastian, Spain.*

[(5)] *Hepatology Programme, Center for Applied Medical Research (CIMA), IDISNA, University of Navarra, Pamplona, Spain.*

[(6)] *Department of Metabolomics, CIC bioGUNE, Technology Park of Vizcaya, Vizcaya, Spain.*

[(7)] *National Institute for the Study of Liver and Gastrointestinal Diseases (CIBERehd), Carlos III National Health Institute, Madrid, Spain.*

Author for correspondence:

Jose J. G. Marin
Department of Physiology and Pharmacology
Campus Miguel de Unamuno E.I.D. S-09
37007-Salamanca, Spain
Telephone: 34-663182872
Fax: 34-923-294669
E-mail: jjgmarin@usal.es

Short Title: OCT1 in chemoresistance of cholangiocarcinoma

Keywords: Biliary Tumors, Chemoresistance, Chemotherapy, Drug Transport, Targeted Therapy; Tyrosine Kinase Inhibitors.

Abbreviations: CCA, cholangiocarcinoma; DAC, decitabine (5-aza-2'-deoxycytidine); DHE, dihydroethidium; eCCA, extrahepatic CCA; HCC, hepatocellular carcinoma; HDAC, histone deacetylases; HDACIs, HDAC inhibitors; iCCA, intrahepatic CCA; MOC, mechanism of chemoresistance; MOI, multiplicity of infection; NT, non-tumor; OCT1, organic cation transporter 1; RBPs, RNA binding proteins; T, tumor; TAA, thioacetamide; TCGA, The Cancer Genome Atlas; TEA, tetraethylammonium; TKI, tyrosine kinase inhibitor; TSA, trichostatin A; TSS, transcriptional start site; UTR, untranslated region.

Funding

This study was supported by the Carlos III Institute of Health, Spain (Grants PI15/00179, PI16/00598 and PI18/01075 co-financed by European Regional Development Fund); Ministry of Science and Innovation, Spain (SAF2013-40620-R and SAF2016-75197-R); "Asociación Española Contra el Cancer", Spain (AECC-2017); "Junta de Castilla y León", Spain (SA015U13 and SA063P17); "Fundación Samuel Solórzano Barruso, Spain (FS/10-2014, FS/08-2017 and FS/13-2017); and "Fundación Mutua Madrileña", Spain (Call 2015). Fundación Vasca de Innovación e Investigación Sanitarias, Spain (Bioef BIO15/CA/011). Ministerio de Economía, Industria y Competitividad, Spain (SAF2017-87301-R); Gobierno Vasco-Departamento de Salud, Spain (2013111114); Basque Foundation for Innovation and Health Research: EiTB Maratoia, Spain (BIO15/CA/016/BD). MA and MAP were supported by a pre-doctoral contract by "Ministry of Education, Culture and Sports", Spain (BOE-A-2015-9456). RAA was supported by a pre-doctoral contract funded by the "Junta de Castilla y León, Fondo Social Europeo" (EDU/828/2014). JBA is supported by the Danish Cancer Society (R98-A6446); Novo Nordisk Foundation (14040); PMG: European Association for the Study of the Liver (EASL) individual Sheila Sherlock Postdoc Fellowship, Marie Sklodowska-Curie Fellowships (MirChol and Epi-Target). CJO is funded by MSCA postdoc fellowship.

Authors contributions

Study concept and design: EL, RIRM, RAA, OB, JJGM

Experimental studies: EL, RAA, MJM, OB, RIRM, SDC, LSV, MAP, MA, PMG, LS, CJO

Data acquisition: EL, RAA, MJM, OB, RIRM, SDC, LSV, MAP, MA, PMG, LS, CJO

Statistical analysis: CJO, EL, JJGM

Interpretation of data: JJGM, EL, JBA, JMB, MAA, MLMC, RIRM

Obtained funding: JJGM, OB, RIRM, JBA, JMB, MAA, MLMC

Drafting of the manuscript: JJGM, EL

Competing interests

None.

ABSTRACT

Although the multi-tyrosine kinase inhibitor, sorafenib is useful in the treatment of several cancers, cholangiocarcinoma (CCA) is refractory to this drug. Among other mechanisms of chemoresistance impaired uptake via hOCT1 (gene *SLC22A1*) has been suggested. Here we have investigated the events accounting for this phenotypic characteristic and have evaluated the interest of selective gene therapy strategies to overcome this limitation. Gene expression and DNA methylation of *SLC22A1* were analyzed using intrahepatic (iCCA) and extrahepatic (eCCA) biopsies (Copenhagen and Salamanca cohorts; n=132) and TCGA-CHOL (n=36). Decreased *hOCT1* mRNA correlated with hypermethylation status of the *SLC22A1* promoter. Treatment of CCA cells with decitabine (demethylating agent) or butyrate (histone deacetylase inhibitor) restored hOCT1 expression and increased sorafenib uptake. MicroRNAs able to induce *hOCT1* mRNA decay were analyzed in paired samples of TCGA-CHOL (n=9) and Copenhagen (n=57) cohorts. Consistent upregulation in tumor tissue was found for miR-141 and miR-330. High proportion of aberrant *hOCT1* mRNA splicing in CCA was also seen. Lentiviral-mediated transduction of eCCA (EGI-1 and TFK-1) and iCCA (HuCCT1) cells with hOCT1 enhanced sorafenib uptake and cytotoxic effects. In chemically-induced CCA in rats reduced rOct1 expression was accompanied by impaired sorafenib uptake. In xenograft models of eCCA cells implanted in mouse liver, poor response to sorafenib was observed. However, tumor growth was markedly reduced by co-treatment with sorafenib and adenoviral vectors encoding hOCT1 under the control of the *BIRC5* promoter, a gene highly upregulated in CCA. ***Conclusions***: The reason for impaired hOCT1-mediated sorafenib uptake by CCA is multifactorial. Gene therapy capable of selectively inducing hOCT1 in tumor cells can be considered a potentially useful chemosensitization strategy to improve the response of CCA to sorafenib.

Introduction

Biliary tract cancers are a type of heterogeneous tumors that include cholangiocarcinoma (CCA) both intrahepatic (iCCA) and extrahepatic (eCCA), and gallbladder cancer, with diverse phenotypic characteristics (1). CCA, whose incidence is increasing worldwide, is currently the second most frequent primary hepatic malignancy after hepatocellular carcinoma (HCC). Surgical resection constitutes the best option for complete cure. However, owing to the lack of accurate non-invasive CCA markers and to the fact that these tumors grow up asymptomatically, they are often detected at an unresectable advanced stage (2, 3). This partly accounts for the very poor prognosis of this cancer, from which most patients die within twelve months after diagnosis. Classical chemotherapy offers a 5-year survival rate lower than 10%, which is due to the negligible degree of response of all types of CCA to available chemotherapeutic regimens (4, 5). Gemcitabine plus cisplatin has become the reference regimen for systemic chemotherapy in patients with biliary tract cancers (6), nonetheless this chemotherapy is poorly effective. Therefore, it is essential to understand the molecular bases of the strong chemoresistance of CCA and to seek for new therapeutic approaches. Despite their heterogeneity regarding several clinical and biological aspects, biliary cancers share their marked chemoresistance. Among the so-called targeted therapies, sorafenib, a multitargeted tyrosine kinase inhibitor (TKI) that blocks the activity of Raf serine/threonine kinase isoforms, as well as VEGFR-2/3, PDGFR, c-KIT, FLT-3 and RET, to inhibit tumor angiogenesis and tumor cell proliferation (7, 8), has been approved for the treatment of HCC (9). Sorafenib is one of the few TKIs that is active even against mutated BRAF, which appears with a high frequency in CCA, especially in iCCA. Moreover, sorafenib has been reported to have some anticancer activity against CCA in experimental models both *in vitro* and *in vivo*, which has not been consistently confirmed in clinical studies (10-14). The lack of response of CCA patients to sorafenib may be the result of the combined action of several mechanisms of chemoresistance (MOCs) (5). We have previously demonstrated that the organic cation transporter 1 (hOCT1, *SLC22A1* gene) can play a key role in sorafenib effectiveness because the mechanism of action of this drug depends on its access to the intracellular domains of the tyrosine kinases that are inhibited by sorafenib (15). Moreover, hOCT1 mediates the uptake of this drug by target cells (15). Of note, it has been demonstrated that decreased expression of hOCT1 constitutes a shared characteristic of liver tumors (HCC, CCA and hepatoblastoma) (16). In addition, not all synthesized *hOCT1* mRNA is translated into functional protein because of the high proportion of inactive variants that are generated as a result of alternative splicing mechanisms or SNPs (15).

In the present study we have evaluated the hypothesis that mechanisms that cause impaired hOCT1 expression/function in CCA may be involved in the lack of response of these tumors to sorafenib and we have investigated the usefulness of epigenetic manipulation and gene therapy in order to sensitize CCA to this drug by selectively enhancing hOCT1 expression in cancer cells under the control of a tumor-specific promoter.

Materials and Methods

Human Samples and Data. Whole transcriptome profiling was performed using human *Ref-8v2 BeadChips* (Illumina) on 68 iCCA and 36 eCCA surgical specimens (T) and 60 samples from adjacent non-tumor tissue (NT), as previously described (GEO: GSE26566) ("Copenhagen cohort" of patients) (17). For a subset of these patients (T=48, NT=41), DNA methylation profiling was performed using *Infinium HumanMethylation27 BeadChip* (Illumina). The methylation status of the hOCT1 promoter was measured using beta (β)-value metric (range: 0-1; 0%-100% methylation) (see detailed description in Supporting Information). To further investigate the degree of DNA hypermethylation in hOCT1, level 1 *Infinium HumanMethylation450 BeadChip* (Illumina Inc.) data (T=36 and NT=9) obtained from TCGA-CHOL consortium (18) were analyzed. For an extended subset of the "Copenhagen cohort", miRNA-sequencing (miR-seq) data were also available for 57 paired T and NT samples and 22 normal livers. For some analyses we have used specimens of iCCA (n=16) and eCCA (n=12) and paired NT samples (n=17) obtained after tumor resection at University Hospital of Salamanca ("Salamanca cohort", see Supporting Table 1). Research protocols were approved by the Ethical Committees for Clinical Research of supporting Institutions, and all patients signed written consents for the use of their samples for biomedical research.

Animals and in vivo Experiments. Male Wistar rats (University of Salamanca Animal House) and female nude mice (Swiss *nu/nu*) (Charles River Laboratories, Barcelona) were used. Nude mice were maintained under pathogen-free environment and handled under stringent sterile conditions. The animals were fed on standard rat or mouse chow (Panlab, Madrid) and water *ad libitum*. Temperature (20°C) and the light/dark cycle (12 h:12 h) were controlled and the protocols were approved by the Ethical Committee of the University of Salamanca. To study sorafenib uptake by CCA, this tumor was induced in rats by including 0.05% thioacetamide (TAA) in the drinking water for 30 weeks (19) (Supporting Information). Xenografts of CCA in nude mice were generated by subcutaneous injection of ≈1x10^6 human EGI-1 eCCA cells to donor nude mice under isoflurane anesthesia. EGI-1 cells were selected due to their acceptable tumorigenesis ability *in vivo* as compared with TFK1 and HuCCT1 cells. Seven weeks later, generated CCA tumors were resected and dissected into ~1 mm^3 pieces that were implanted under anesthesia in the livers of several host nude mice (20). The following day, the animals were randomly divided into 4 groups for the co-administration of control adenoviruses (Ad-Mock: Ad-BIRC5pr-EGFP) or adenoviruses containing Ad-BIRC5pr-hOCT1-EGFP plus sorafenib or the vehicle alone (saline). Additional control mice

were used to measure serum levels of routine biochemical parameters for comparative purposes. Adenoviral particles were injected every 5 days ($4x10^7$ VP/mice in each administration, i.v. through the tail vein). Sorafenib (10 mg/kg b.w.) or saline were administered (i.p.) twice per week. At the end of the experiment (after 2 months), the animals were anesthetized with sodium pentobarbital to measure the tumor volume and to collect tissues and blood samples. Serum levels of routine biochemical parameters were determined in a dry chemistry automated analyzer Spotchem EZ SP-4430 (Arkray Factory, A. Menarini Diagnostics, Badalona, Spain).

Lentiviral and Adenoviral Vectors. The human OCT1 ORF was amplified from total RNA isolated from healthy liver by reverse transcription followed by high-fidelity PCR using AccuPrime Pfx DNA polymerase (Life Technologies) and specific primers (Supporting Table 2). OCT1 cDNA was cloned into the *Pac*I site of the pWPI lentiviral vector (that contains the constitutive EF1α promoter). Recombinant lentiviruses production and lentiviral transduction are described in Supporting Information.

The promoter region of the *BIRC5* gene (*BIRC5pr*, 1467-bp zone of the 5′-flanking region) was cloned from human hepatoma PLC/PRF/5 (Alexander) cells using AccuPrime Pfx DNA polymerase, and specific oligonucleotide primers (Supporting Table 2). The cloning procedure is described in detail in Supporting Information.

In vitro Experiments. Cells transduced with lentiviral vectors (Lent-MOCK or Lent-OCT1) were seeded onto 96-well plates at subconfluence (5,000 to 7,500 cells/dish). After 24 h the cells were exposed to 5 μM sorafenib for 6 h. The formazan test using thiazolyl blue tetrazolium bromide (Sigma-Aldrich) was used to determine cell viability 66 h later.

The transport function of hOCT1 was measured by the uptake of organic cations, such as dihydroethidium (DHE, 5 μM) by flow cytometry and [^{14}C]-TEA (150 μM) by radioactivity determination. Specific hOCT1 inhibition was determined using quinine (250 μM). Sorafenib (5 μM) uptake was also determined using an adaptation of a previously published method using HPLC-MS/MS (15). In uptake experiments, the results were corrected by protein content (21).

The role of miRNAs potentially involved in regulating hOCT1 expression was studied in EGI-1 and TFK-1 cells, using lentivirus designed to mimic the pre-miRNA (hsa-mir-141/330/1468) sequence including the loop (Supporting Information).

Quantitative RT-PCR (RT-QPCR). Total RNA extraction from cells and tissues and retro-transcription were performed as previously described (16) (Supporting Information). The primer oligonucleotide sequences to carry out QPCR are described in Supporting Table 3.

The results of mRNA abundance of target genes in each sample were normalized on the basis of *GAPDH*, *HPRT1* or *rat ACTB* (β-actin) mRNA abundance.

Immunofluorescence and Immunoblotting Assays. Immunofluorescent staining was performed on tissue cryosections air-dried and fixed in cold methanol using appropriate antibodies against hOCT1, PECAM1 and Na^+/K^+-ATPase. Nuclei were counterstained with DAPI. Confocal laser-scanning microscopy was performed using a Leica TCS SP2 confocal microscope. Immunoblotting analyses of cell lysates were carried out in 12% SDS-PAGE, loading 30 μg of protein per lane. Appropriate primary antibodies for survivin and GAPDH were diluted in PBS-Tween. Immunoreactive protein bands were visualized by ECL (Amersham Pharmacia Biotech) after incubation with appropriate secondary antibodies (IgG-HRP linked). See Supporting Information for antibodies characteristics and conditions of antibodies.

Determination of Alternative Splicing. Based on previous reports of alternative spliced hOCT1 variants (15), we designed primers annealing in exon 6 (Forward) and exon 11 (Reverse) that are shared by all hOCT1 isoforms (Supporting Table 3). PCR was carried out with Platinum-Taq DNA polymerase (Life Technologies) using 30 cycles of amplification. The presence and size of the PCR products were determined by gel electrophoresis and a semi-quantitative determination of the amount of each splicing variant was carried out by densitometry of the bands using a LAS-4000 luminescent image analyzer.

Statistical Analyses. Results were statistically analyzed using *GraphPad* program. For comparisons between two groups, parametric paired t-test or *t-Student* test and non-parametric *Mann-Whitney* test were used. After ANOVA, Bonferroni method of multiple-range testing was used to calculate the statistical significance of differences among groups.

Results

Role of DNA Methylation in hOCT1 Downregulation. The relationship between hOCT1 expression and the methylation status of the *SLC22A1* promoter was analyzed in resected CCA specimens from two different cohorts of patients: i) TCGA-CHOL, including TCGA Infinium 450k data and ii) the "Copenhagen cohort". We have confirmed hOCT1 downregulation in CCA *vs.* peritumor tissue in both cohorts (Fig. 1A and 1C). hOCT1 promoter was significantly hypermethylated in CCA (using the probe cg27292431, corresponding to exon 1 of *SLC22A1*) compared to peritumor tissue (Fig. 1B and 1D). Owing to the importance of the location of CpG dinucleotide hypermethylation in relationship to gene expression, we analyzed 450k data from TCGA-CHOL which provides increased hOCT1 promoter coverage. Accordingly, we uncovered three additional hypermethylated probes mapping to the transcriptional start site and 5'-UTR of hOCT1 (Supporting Fig. 1). When, both in the "Copenhagen cohort" (Fig. 1E) and the "Salamanca cohort" (Fig. 1F), hOCT1 expression was analyzed separately in iCCA and eCCA, similar marked downregulation in both types of tumors was found.

In vitro hOCT1 Expression

To investigate the functional impact of *SLC22A1* hypermethylation, CCA cell lines also with markedly reduced *hOCT1* mRNA levels (15, 16), were treated with DAC. This DNA demethylating agent restored hOCT1 expression in EGI-1 (Fig. 2A) and TFK-1 (Fig. 2B) cells. Because acetylation of histones facilitates gene expression and histone deacetylases (HDACs) are overexpressed in CCA cells, which leads to a reduced expression of genes involved in differentiation (22), we evaluated whether HDAC inhibitors (HDACI) could affect *hOCT1* mRNA expression in CCA cells. Sodium butyrate induced hOCT1 upregulation both in EGI-1 (Fig. 2C) and TFK-1 (Fig. 2D) cells. The magnitude of the effect after 5 days of treatment was DAC>butyrate in EGI-1 cells but butyrate>DAC in TFK-1 cells. Other HDACIs, such as phenyl butyrate increased *hOCT1* mRNA levels, but only in TFK-1 cells and to a lesser extent than butyrate, whereas TSA had no significant effect in any of these cell lines (Fig. 2C and 2D). Using EGI-1, in which DAC effect was stronger, it was demonstrated that the recovery of hOCT1 expression was accompanied by enhanced sorafenib uptake (Fig. 2E).

Role of microRNA in hOCT1 Downregulation. In a separate study, we have carried out *in silico* analysis of microRNA-induced *hOCT1* mRNA decay. Among six selected miRs, only three showed activity in HepG2 hepatoma cells (23). Here, we have shown that the same

microRNAs, i.e., 141, 1468 and 330 reduced *hOCT1* mRNA in EGI-1 (Fig. 2F) and TFK-1 (Fig. 2G) cells. The expression of these three microRNAs in paired T and NT specimens from both TCGA-CHOL and the extended "Copenhagen cohort" was analyzed and compared with that of *hOCT1* (Fig. 3). Both miR-141 and miR-330 were consistently upregulated in both groups of CCA. In the same paired specimens, *hOCT1* mRNA was consistently decreased (Fig. 3F and 3L). In contrast, there was a discrepancy between both series regarding changes in miR-1468 expression (Fig. 3B and 3H).

Aberrant Splicing. To quantify the importance of aberrant splicing in overall hOCT1 expression/function we evaluated the presence of splicing variants by PCR using specific primers to amplify the hOCT1 amplicon between the exons 6 and 11 (Fig. 4A). The length of the amplified fragment was used to distinguish wild type from shorter variants (Fig. 4B and 4C). Measurement by densitometry of the abundance of splicing variants revealed higher proportion of aberrant forms in CCA (both in biopsies and in cell lines) than in healthy liver. Interestingly, aberrant splicing was also present in peritumor tissue (Fig. 4D).

Role of mRNA Stability/Decay Proteins. To investigate whether changes in the balance of RNA binding proteins (RBPs) involved in mRNA stability/decay could affect the levels of *hOCT1* mRNA in CCA, the expression of genes involved in mRNA decay (*AUF1, BRF1, BRF2, CUGBP, FBP2*, and *TTP*) or mRNA stability (*HuR*) was measured in paired samples of tumor and peritumor tissue ("Salamanca cohort"). We found no significant difference between T and NT tissue for any of these genes (Supporting Fig. 2A-2F), except for *TTP* (Supporting Fig. 2G), that was downregulated in CCA samples. Similar results were found when the expression levels of RBP genes were determined in CCA cell lines (data not shown).

hOCT1 Downregulation Correlates with Decreased Sorafenib Uptake by CCA Tumors. A rat model of chemically induced CCA (19) was used to study whether downregulation of this transporter results in impaired uptake of sorafenib by CCA tumors *in vivo* (Fig. 5). Sorafenib was intravenously administered to CCA bearing rats. Samples from both T and NT tissue were collected 1 h later and their sorafenib content was determined using HPLC-MS/MS. The results indicated that peritumor tissue, which maintained higher Oct1 levels in comparison with CCA (Fig. 5D), was able to efficiently take up sorafenib (Fig. 5E). In contrast, in the tumors the reduced expression of Oct1 (Fig. 5D) was accompanied with a consistent and significant decrease in sorafenib content (Fig. 5E).

Relationship between hOCT1 Expression and Sorafenib Uptake/Activity. To evaluate whether the experimental overexpression of hOCT1 could be used to increase the cytotoxic effect of sorafenib, eCCA (TFK-1 and EGI-1) and iCCA (HuCCT1) cells were transduced using lentivirus either empty (MOCK) or containing hOCT1 coding sequence (Lent-OCT1). The high efficacy of transduction, as analyzed by counting EGFP positive cells (≈95%, ≈60% and ≈80% in TFK-1, EGI-1 and HuCCT1 cells, respectively), resulted in marked increase in *hOCT1* mRNA expression (Fig. 6A-6C). Consequently, hOCT1 transduced cells showed enhanced ability to take up, in a quinine-sensitive manner, organic cations, such as DHE (Fig. 6D-6F) and TEA (Supporting Fig. 3). Moreover, in comparison with MOCK transduced cells, hOCT1 expressing CCA cells showed higher ability to take up (Fig. 6G-6I) and respond (Fig. 6J-6L) to sorafenib. Enhanced cytotoxic effect of sorafenib in CCA cells overexpressing hOCT1 was consistent with the inhibition of the phosphorylation of the sorafenib-known target STAT3 as revealed by immunoblot analysis (Supporting Fig. 4).

Tumor-Selective Chemosensitization by Gene Therapy. In order to restrict transgene expression to tumor cells we designed an adenoviral vector in which hOCT1 expression was driven by *BIRC5pr*, due to the high activity of this promoter found in clinical CCA specimens (24). As it has been previously reported (16) and we have confirmed here, the levels of both *BIRC5* mRNA and survivin protein were greatly increased in CCA cells compared with healthy liver and normal human cholangiocytes (NHC) (Fig. 7A-B). Promoter activity was evaluated in transfection experiments with Alexander cells using vectors encoding firefly luciferase (Luc2) under the control of either *CMVpr* or *BIRC5pr*. Both promoters were similarly potent stimulating Luc2 expression (Fig. 7C and 7D). Based on these results, adenoviruses bearing *BIRC5pr-EGFP* (Ad-MOCK) (Fig. 7E) or *BIRC5pr-hOCT1-EGFP* (Ad-hOCT1) (Fig. 7F) were used to treat nude mice with intrahepatic CCA xenograft (Fig. 8). Gene therapy resulted in selective overexpression of hOCT1 at the plasma membrane of tumor cells, whereas no detectable expression in adjacent peritumor tissue (Fig. 8C-8F) or endothelial cells (Supporting Fig. 5) was found. In mice treated with Ad-MOCK, sorafenib treatment failed to affect tumor growth (Fig. 8G-8H). In contrast, co-administration of sorafenib plus Ad-hOCT1 resulted in a marked antitumor effect (Fig. 8G-8H), which was not accompanied by decreased vascularization (Supporting Fig. 6). Interestingly, in the absence of treatment with sorafenib, the administration of these vectors did not affect tumor growth. Moreover, signs of renal or hepatic toxicity were not found (Supporting Table 4).

Discussion

At present, sorafenib is the reference drug used in the pharmacological treatment of HCC. The high proportion of genetic alterations in critical signaling pathways involved in cell proliferation in CCA has led to an interest in the development of clinical trials investigating targeted therapies including sorafenib (1). However, data on sorafenib, and other TKIs, effectiveness in CCA patients are controversial, reporting both beneficial effect (12, 25, 26), and poor activity against this type of liver cancer (27, 28). The latter is not surprising considering the strong multidrug resistance (MDR) phenotype of CCA, in which several MOCs involved in the lack of response to sorafenib have been identified (5). These include the overexpression of ABC proteins, such as MDR1 and BCRP, which reduce intracellular drug content (MOC-1b); enhanced drug inactivation by uridine glucuronosyl transferase 1A (MOC-2) or the appearance of genetic variants in the intracellular targets of sorafenib (MOC-3) (29). In addition, we have previously reported that because cell uptake, which is mediated mainly by hOCT1, is an essential requirement for sorafenib to reach its intracellular targets and carry out its pharmacological effect, changes in the expression/activity of this carrier can lead to poorer response to sorafenib (15). As a natural continuation of this line of research, in the present study we have analyzed the causes of hOCT1 downregulation in CCA, and we have explored strategies to restore its expression and hence increase its sensitivity to sorafenib.

We have previously reported that hOCT1 expression is reduced in HCC (16) and CCA (30). In CCA, epigenetic abnormalities, including DNA hypermethylation, have been described (31). Moreover, hypermethylation of *SLC22A1* promoter in HCC has been reported (32), and, as we have demonstrated here, these changes also occur in CCA. An inverse behavior regarding *hOCT1* mRNA expression and hypermethylation status of three critical CpG regions (5'-UTR, TSS and exon 1) has been found. This is consistent with the concept that methylation of the first exon correlates with transcriptional silencing of *SLC22A1* gene (33). Although further studies are needed, our data suggest that methylation of *SLC22A1* could be a prognostic biomarker in CCA as has been proposed in HCC (32).

As suggested by our results, DAC treatment is an efficient strategy to restore OCT1 expression in CCA cell lines, which enhances sorafenib uptake. These findings support that demethylating agents could be useful in restoring hOCT1 expression in CCA tumors and hence improving sorafenib uptake/response. Moreover, clinical data indicate that DAC treatment retards CCA tumor growth (34). Thus, combination therapy of DAC plus sorafenib

should be explored in CCA patients. In support of this view, treatment of acute myeloid leukemia with DAC plus sorafenib has shown synergistic antitumor effect (35).

Although the upregulation induced by DAC in EGI-1 cells was strong (≈15-fold) (Fig. 2A), the impact of this change in the functional experiments was modest (Fig. 2E). This could be partly due to the fact that a fraction of the synthesized hOCT1 pre-mRNA was processed to inactive variants by an aberrant splicing that was quantitatively important both in CCA tumors and cell lines (Fig. 4C). In a previous study on a low number of specimens of CCA, several variants of aberrant splicing of *hOCT1* pre-mRNA were identified (15). This is pharmacologically relevant because these variants encode truncated non-functional proteins. Interestingly, here we have found aberrant variants both in tumor and peritumor tissues, while this was negligible in healthy liver. The presence of enhanced alternative splicing in the mRNA of some genes has been described to occur during early stages of several liver diseases (36). An ongoing study on liver samples from patients with different liver diseases, without cancer, suggests a heterogeneous degree of aberrant splicing of *hOCT1* pre-mRNA, which is lower than in CCA (data not shown).

Other epigenetic mechanisms, such as histone deacetylation, although to a less extend, seem to also play a role in the modulation of hOCT1 expression. RBPs, that bind AU-rich elements in the 3′ UTR of many mRNAs and target them for stabilization or rapid decay (37), might also be involved in *hOCT1* mRNA decay. As the only change observed was a decreased expression of TTP, which participates in mRNA decay, our results do not support a role of RBPs in *hOCT1* mRNA downregulation. However, this cannot be ruled out because the complex regulation of the function of RBPs has not been explored in depth here. In contrast, *in vitro* activity measurements together with analysis of microRNA expression in CCA samples suggest a possible role of miR-141 and miR-330 in *hOCT1* mRNA modulation in CCA.

Although epigenetic therapies such as DAC administration may be useful for recovering *hOCT1* mRNA levels, the generation of aberrant isoforms and the presence of inactivating SNPs that appear in CCA (15) would limit the gaining of hOCT1 function. In contrast, *in vitro* studies clearly demonstrate that enhanced expression of exogenous hOCT1 results in higher sorafenib uptake and sensitivity. One of the mechanisms accounting for sorafenib antitumor activity involves inhibition of survival JAK/STAT3 signaling pathway that includes reduced STAT3 phosphorylation (10, 38). Immunoblot analysis revealed that treatment of TFK-1 cells with sorafenib induced a marked reduction in the proportion of phosphorylated STAT3 only if the cells over-expressed hOCT1 (Supporting Fig. 4).

Prompted by these findings, we have evaluated the alternative of inducing hOCT1 expression by viral transduction in CCA cells. Thus, as a proof of concept, we have assayed an *in vivo* strategy of gene therapy using adenoviruses, which can infect a broad range of human cells with high gene transfer efficiency (39, 40), and have been proposed for the treatment of neoplastic diseases, including CCA (41). We have used adenoviruses serotype 5 (Ad5), which has become the most popular system in virotherapy. The fact that Ad5 has hepatotropic properties is an advantage for targeting this organ, but it could be a partial obstacle for its successful application in liver tumors such as CCA. To overcome this problem we have used a transcriptional targeting strategy that exploits the activity of tumor-specific promoters that are preferentially active in tumor cells in comparison with normal cells (42). Survivin (*BIRC5* gene), a member of the inhibitor of apoptosis family that is involved in controlling mitotic progression and preventing cell death, is overexpressed in many cancers including CCA, but not in normal adult tissues (43-45). Previous studies have suggested the interest of *BIRC5pr* for tumor-targeted therapy (46) due to its high tumor activity, as high as *CMVpr* (Fig. 7), and low activity in healthy cells (47). This accounts for the specific transduction reached in the experimental model of orthotopic CCA xenograft. Accordingly, the expression of hOCT1 at the plasma membrane of tumor cells dramatically improved the antitumor effect of sorafenib.

Taken together, our study demonstrates that events such as promoter hypermethylation, microRNA-mediated degradation and aberrant splicing, lead to decreased *hOCT1* mRNA and sorafenib uptake/response in CCA. Gene therapy able to selectively induce hOCT1 expression in tumor cells, but not in adjacent healthy liver tissue, is a useful chemosensitizating strategy to improve the response of CCA to sorafenib.

Figure Legends

Fig. 1. hOCT1 expression and promoter methylation in CCA. Levels of *hOCT1* mRNA determined by microarray (A,C) and methylation status (B,D) in tumors (T) compared to paired non-tumor tissue (NT) analyzed in TCGA-CHOL (A,B) (NT, n=9; T, n=36) and Copenhagen cohort (C,D) (NT, n=60; T, n=104). Methylation was determined using cg27292431 probe at exon 1 of *SLC22A1*. Values are individual measurements of T (open triangles) and NT (open circles) samples or mean±SD (solid lines). Comparison between T and NT was carried out using Mann-Whitney t-test. RPKM, reads per kilobase mapped; A.U., arbitrary units. Separate analysis of hOCT1 expression in intrahepatic (iCCA) and extrahepatic (eCCA) tumors and adjacent non-tumor liver tissue (NT) in the Copenhagen cohort (iCCA, n=68; eCCA, n=36; NT, n=60) (E) and the Salamanca cohort (iCCA, n=16; eCCA, n=12; NT, n=17) (F). Values are represented as mean±SD.

Fig. 2. Effect of hypomethylating agents and histone deacetylase inhibitors on hOCT1 expression/function. *hOCT1* mRNA levels in EGI-1 (A) and TFK-1 (B) CCA cells were measured after exposure to 1 μM of decitabine (DAC) for 3, 5 or 7 days. In Control groups, a similar amount of the vehicle (DMSO) alone was added to the culture medium. *hOCT1* mRNA levels in EGI-1 (C) and TFK-1 (D) CCA cells after incubation with histone deacetylase inhibitors: 5 mM sodium butyrate, 5 mM phenyl butyrate or 150 nM trichostatin A (TSA). To evaluate the effect of DAC treatment (1 μM for 5 days) on the ability of EGI-1 cells to take up sorafenib, EGI-1 cells where incubated with 5 μM sorafenib with or without 250 μM quinine for 1 h and its levels in the cells were measured by HPLC-MS/MS (E). Evaluation of the ability of three miRNAs to induce *hOCT1* mRNA decay in EGI-1 (F) and TFK-1 (G) cells. CCA cells were transduced with lentiviral vectors able to induce the expression of short-hairpin RNA against luciferase (sh-Luc2, Control), or against hOCT1 (sh-hOCT1), or one of the three miRNA selected from their predicted interaction with pre-mRNA by *in silico* analysis, and one day after transduction cells were treated with 1 μM DAC for 5 days to maximize hOCT1 expression. Values are mean±SD (n=4). *, $p<0.05$ upon comparing with control. †, $p<0.05$ upon comparing with results obtained in absence of quinine.

Fig. 3. Expression of microRNAs with potential role in *hOCT1* mRNA modulation in CCA. Individual values of expression levels of miR-141 (A), miR-1468 (B), miR-330 (C), and *hOCT1* mRNA (D) in 9 paired samples of tumor tissue (T) and adjacent non-tumor tissue (NT) as downloaded from TCGA-CHOL (A-F). Similar analysis was carried out on 57 paired T and NT samples and 22 normal livers included in the Copenhagen cohort (G-L). Average

values (mean±SEM) and statistical comparisons are shown in E, F, K and L. ***, p<0.001, on comparing T and NT by paired *t*-test. RPKM, reads per kilobase mapped; RPMM, reads per million miRNA mapped.

Fig. 4. Alternative splicing of human *hOCT1* mRNA in CCA. Scheme of human *OCT1* pre-mRNA showing exons (1-11 boxes), introns (horizontal lines) and untranslated regions (striped boxes). Dashed lines indicate exon skipping or intron retention variants due to aberrant splicing. The locations of forward (Fw) and reverse (Rv) primers used to detect spliced forms are depicted (A). Expected size of amplicons resulting from PCR using Fw and Rv primers (B). Representative separation by gel electrophoresis of PCR products obtained using as template: complete *hOCT1* mRNA (from a plasmid), CCA tumor tissue, and CCA cells (EGI-1 and TFK-1) (C). Densitometric analysis of the semi-quantitative PCR of spliced forms of *hOCT1* mRNA in healthy liver, paired peritumor tissue (NT, n=5) and CCA tumor tissue (T, n=9) (D). WT= Wild type OCT1; SP = Aberrant splicing. *, p<0.05, on comparing T or NT with healthy liver. Comparison of T with NT was p>0.05.

Fig. 5. Relationship between rOct1 expression and sorafenib uptake in rat CCA. Macroscopic view of tumors (A, arrow) and histological images by hematoxylin and eosin staining under light-field microscope with 10x magnification of adjacent liver parenchyma (B) and tumor tissue (C) in rats after 30 weeks of continuous administration of 0.05% thioacetamide (TAA) in the drinking water. Relative expression of rOct1 in non-tumor (NT) liver tissue and paired tumors (T) of rats (n=12) with chemically-induced CCA (D). Sorafenib content (measured by HPLC-MS/MS) in T (n=15) and NT (n=10) tissues 60 min after administration of sorafenib (10 mg/kg b.w., i.v.) (E). Results are shown as individual values (circles) or as means±SD (squares). *, p<0.05, on comparing T with NT.

Figure 6. Role of hOCT1 in sorafenib uptake and response *in vitro*. Extrahepatic (TFK-1 and EGI-1) and intrahepatic (HuCCT1) CCA cells were transduced with control lentivirus (MOCK) or hOCT1 lentivirus (Lent-OCT1). Relative *hOCT1* mRNA levels (A-C) were evaluated in WT, MOCK or OCT1 transduced cells. Measurements were carried out 4 days after transduction. MOCK or Lent-OCT1 CCA cells were incubated with 5 μM dihydroethidium (DHE) in the absence (Control) or the presence of 250 μM quinine for 15 min to determine hOCT1 function (D-F). MOCK or Lent-OCT1 CCA cells were incubated with 5 μM sorafenib for 1 h and its levels in the cells were measured by HPLC-MS/MS (G-I). Cell viability (J-L) was evaluated in MOCK or Lent-OCT1 CCA after incubation with 5 μM sorafenib for 6 h, and cell viability was measured 66 h later to evaluate sorafenib response. Values are mean±SD from 9 wells of 3 different cultures in each cell line. *, p<0.05, on comparing with MOCK cells.

†, p<0.05, on comparing cells incubated with quinine (D, E, F) or sorafenib (J, K, L) with their corresponding Control groups.

Fig. 7. Tumor-Selective Gene Therapy Strategy Design. Relative levels of *BIRC5* mRNA in NHC (normal human cholangiocytes), EGI-1 and TFK-1 CCA cells, and in Alexander HCC cells (A). Representative immunoblots of survivin and GAPDH in human hepatocytes, healthy liver, and CCA cell lines (EGI-1 and TFK1) (B). Representative experiment (C) and average values (D) of *BIRC5* promoter (*BIRC5pr*) activity determined 48 h after transient transfection of Alexander cells with *BIRC5pr-Luc2*, *CMVpr-Luc2* or *pL-Luc2* (negative control, without promoter) plasmids. Values are mean±SD from at least 3 experiments performed in triplicate. *, p<0.01, as compared to pL-Luc2. N.S., no significant differences. ALU, arbitrary luminescence units. Partial scheme of control adenovirus *Ad-prBIRC5-EGFP* (Ad-MOCK) (E) and adenoviral vector containing *hOCT1* ORF (*Ad-prBIRC5-hOCT1*) (F).

Fig. 8. Antitumor effect of sorafenib on xenograft CCA tumors selectively expressing hOCT1. Nude mice were used to generate subcutaneous CCA tumors with EGI-1 cells. These were used as donors for subsequent intrahepatic implantation in different animals. Histological appearance of adjacent non-tumor tissue (A), and CCA tumor tissue (B) as observed by hematoxylin and eosin staining under light-field microscope with 10x magnification. These animals were treated with adenoviruses injected every 5 days (i.v. via tail vein at $4x10^7$ VP/mice in each administration). Adenoviral vector *Ad-prBIRC5-hOCT1* was used to induce hOCT1 expression as seen by immunofluorescence detection by confocal microscopy (cyanin-5 fluorescence was artificially converted into green) (C, D). Na^+/K^+-ATPase (red) was used as a plasma membrane marker in adjacent non-tumor liver tissue (E) and implanted CCA tumors (F). The insets are amplified details of merge images showing the nuclei stained with DAPI (blue). Animal injected with *Ad-prBIRC5-hOCT1* (Ad-hOCT1) or control *Ad-prBIRC5-EGFP* (Ad-MOCK) vectors were treated with saline or sorafenib (10 mg/kg b.w, i.p. twice a week). Representative images of gross appearance of livers of a mouse from each group showing the implanted tumor (G, arrows). Tumor volume was determined at the end of the experimental period (2 months), when the animals were slaughtered and tumors were excised and measured (H). Values are mean±SD from four experimental groups; Ad-MOCK+saline (n=5), Ad-MOCK+sorafenib (n=6), Ad-OCT1+saline (n=4), Ad-OCT1+sorafenib (n=7). *, p<0.05, on comparing the Ad-OCT1 group treated with sorafenib with the group that received saline alone.

References

1. Ahn DH, Bekaii-Saab T. Biliary cancer: intrahepatic cholangiocarcinoma vs. extrahepatic cholangiocarcinoma vs. gallbladder cancers: classification and therapeutic implications. J Gastrointest Oncol 2017;8:293-301.

2. Lazaridis KN, Gores GJ. Cholangiocarcinoma. Gastroenterology 2005;128:1655-1667.

3. Banales JM, Cardinale V, Carpino G, Marzioni M, Andersen JB, Invernizzi P, Lind GE, et al. Expert consensus document: Cholangiocarcinoma: current knowledge and future perspectives consensus statement from the European Network for the Study of Cholangiocarcinoma (ENS-CCA). Nat Rev Gastroenterol Hepatol 2016;13:261-280.

4. Khan SA, Davidson BR, Goldin RD, Heaton N, Karani J, Pereira SP, Rosenberg WM, et al. Guidelines for the diagnosis and treatment of cholangiocarcinoma: an update. Gut 2012;61:1657-1669.

5. Marin JJG, Lozano E, Herraez E, Asensio M, Di Giacomo S, Romero MR, Briz O, et al. Chemoresistance and chemosensitization in cholangiocarcinoma. Biochim Biophys Acta 2018;1864:1444-1453.

6. Valle J, Wasan H, Palmer DH, Cunningham D, Anthoney A, Maraveyas A, Madhusudan S, et al. Cisplatin plus gemcitabine versus gemcitabine for biliary tract cancer. N Engl J Med 2010;362:1273-1281.

7. Wilhelm S, Carter C, Lynch M, Lowinger T, Dumas J, Smith RA, Schwartz B, et al. Discovery and development of sorafenib: a multikinase inhibitor for treating cancer. Nat Rev Drug Discov 2006;5:835-844.

8. Carlomagno F, Anaganti S, Guida T, Salvatore G, Troncone G, Wilhelm SM, Santoro M. BAY 43-9006 inhibition of oncogenic RET mutants. J Natl Cancer Inst 2006;98:326-334.

9. Llovet JM, Ricci S, Mazzaferro V, Hilgard P, Gane E, Blanc JF, de Oliveira AC, et al. Sorafenib in advanced hepatocellular carcinoma. N Engl J Med 2008;359:378-390.

10. Sugiyama H, Onuki K, Ishige K, Baba N, Ueda T, Matsuda S, Takeuchi K, et al. Potent in vitro and in vivo antitumor activity of sorafenib against human intrahepatic cholangiocarcinoma cells. J Gastroenterol 2011;46:779-789.

11. Huether A, Hopfner M, Baradari V, Schuppan D, Scherubl H. Sorafenib alone or as combination therapy for growth control of cholangiocarcinoma. Biochem Pharmacol 2007;73:1308-1317.

12. LaRocca RV, Hicks MD, Mull L, Foreman B. Effective palliation of advanced cholangiocarcinoma with sorafenib: a two-patient case report. J Gastrointest Cancer 2007;38:154-156.

13. Pan TT, Wang W, Jia WD, Xu GL. A single-center experience of sorafenib monotherapy in patients with advanced intrahepatic cholangiocarcinoma. Oncol Lett 2017;13:2957-2964.

14. Luo X, Jia W, Huang Z, Li X, Xing B, Jiang X, Li J, et al. Effectiveness and safety of sorafenib in the treatment of unresectable and advanced intrahepatic cholangiocarcinoma: a pilot study. Oncotarget 2017;8:17246-17257.

15. Herraez E, Lozano E, Macias RI, Vaquero J, Bujanda L, Banales JM, Marin JJ, et al. Expression of SLC22A1 variants may affect the response of hepatocellular carcinoma and cholangiocarcinoma to sorafenib. Hepatology 2013;58:1065-1073.

16. Martinez-Becerra P, Vaquero J, Romero MR, Lozano E, Anadon C, Macias RI, Serrano MA, et al. No correlation between the expression of FXR and genes involved in multidrug resistance phenotype of primary liver tumors. Mol Pharm 2012;9:1693-1704.

17. Andersen JB, Spee B, Blechacz BR, Avital I, Komuta M, Barbour A, Conner EA, et al. Genomic and genetic characterization of cholangiocarcinoma identifies therapeutic targets for tyrosine kinase inhibitors. Gastroenterology 2012;142:1021-1031 e1015.

18. Farshidfar F, Zheng S, Gingras MC, Newton Y, Shih J, Robertson AG, Hinoue T, et al. Integrative Genomic Analysis of Cholangiocarcinoma Identifies Distinct IDH-Mutant Molecular Profiles. Cell Rep 2017;18:2780-2794.

19. Lozano E, Sanchez-Vicente L, Monte MJ, Herraez E, Briz O, Banales JM, Marin JJ, et al. Cocarcinogenic effects of intrahepatic bile acid accumulation in cholangiocarcinoma development. Mol Cancer Res 2014;12:91-100.

20. Dominguez MF, Macias RI, Izco-Basurko I, de La Fuente A, Pascual MJ, Criado JM, Monte MJ, et al. Low in vivo toxicity of a novel cisplatin-ursodeoxycholic derivative (Bamet-UD2) with enhanced cytostatic activity versus liver tumors. J Pharmacol Exp Ther 2001;297:1106-1112.

21. Markwell MA, Haas SM, Bieber LL, Tolbert NE. A modification of the Lowry procedure to simplify protein determination in membrane and lipoprotein samples. Anal Biochem 1978;87:206-210.

22. Morine Y, Shimada M, Iwahashi S, Utsunomiya T, Imura S, Ikemoto T, Mori H, et al. Role of histone deacetylase expression in intrahepatic cholangiocarcinoma. Surgery 2012;151:412-419.

23. Al-Abdulla R, Lozano E, Macias RIR, Monte MJ, Briz O, O'Rourke CJ, Serrano MA, et al. Epigenetic events involved in organic cation transporter 1-dependent impaired response of hepatocellular carcinoma to sorafenib. Br J Pharmacol 2018.

24. Zhu ZB, Chen Y, Makhija SK, Lu B, Wang M, Rivera AA, Yamamoto M, et al. Survivin promoter-based conditionally replicative adenoviruses target cholangiocarcinoma. Int J Oncol 2006;29:1319-1329.

25. Pinter M, Sieghart W, Reisegger M, Wrba F, Peck-Radosavljevic M. Sorafenib in unresectable intrahepatic cholangiocellular carcinoma: a case report. Wien Klin Wochenschr 2011;123:61-64.

26. Chakunta HR, Sunderkrishnan R, Kaplan MA, Mostofi R. Cholangiocarcinoma: treatment with sorafenib extended life expectancy to greater than four years. J Gastrointest Oncol 2013;4:E30-32.

27. El-Khoueiry AB, Rankin CJ, Ben-Josef E, Lenz HJ, Gold PJ, Hamilton RD, Govindarajan R, et al. SWOG 0514: a phase II study of sorafenib in patients with unresectable or

metastatic gallbladder carcinoma and cholangiocarcinoma. Invest New Drugs 2012;30:1646-1651.

28. Bengala C, Bertolini F, Malavasi N, Boni C, Aitini E, Dealis C, Zironi S, et al. Sorafenib in patients with advanced biliary tract carcinoma: a phase II trial. Br J Cancer 2010;102:68-72.

29. Rosenzweig SA. Acquired resistance to drugs targeting receptor tyrosine kinases. Biochem Pharmacol 2012;83:1041-1048.

30. Lozano E, Monte MJ, Briz O, Hernandez-Hernandez A, Banales JM, Marin JJ, Macias RI. Enhanced antitumour drug delivery to cholangiocarcinoma through the apical sodium-dependent bile acid transporter (ASBT). J Control Release 2015;216:93-102.

31. Jusakul A, Cutcutache I, Yong CH, Lim JQ, Huang MN, Padmanabhan N, Nellore V, et al. Whole-Genome and Epigenomic Landscapes of Etiologically Distinct Subtypes of Cholangiocarcinoma. Cancer Discov 2017;7:1116-1135.

32. Schaeffeler E, Hellerbrand C, Nies AT, Winter S, Kruck S, Hofmann U, van der Kuip H, et al. DNA methylation is associated with downregulation of the organic cation transporter OCT1 (SLC22A1) in human hepatocellular carcinoma. Genome Med 2011;3:82.

33. Brenet F, Moh M, Funk P, Feierstein E, Viale AJ, Socci ND, Scandura JM. DNA methylation of the first exon is tightly linked to transcriptional silencing. PLoS One 2011;6:e14524.

34. Wang B, Li H, Yang R, Zhou S, Zou S. Decitabine inhibits the cell growth of cholangiocarcinoma in cultured cell lines and mouse xenografts. Oncol Lett 2014;8:1919-1924.

35. Muppidi MR, Portwood S, Griffiths EA, Thompson JE, Ford LA, Freyer CW, Wetzler M, et al. Decitabine and Sorafenib Therapy in FLT-3 ITD-Mutant Acute Myeloid Leukemia. Clin Lymphoma Myeloma Leuk 2015;15 Suppl:S73-79.

36. Webster NJG. Alternative RNA Splicing in the Pathogenesis of Liver Disease. Front Endocrinol (Lausanne) 2017;8:133.

37. Sanchez-Diaz P, Penalva LO. Post-transcription meets post-genomic: the saga of RNA binding proteins in a new era. RNA Biol 2006;3:101-109.

38. Blechacz BR, Smoot RL, Bronk SF, Werneburg NW, Sirica AE, Gores GJ. Sorafenib inhibits signal transducer and activator of transcription-3 signaling in cholangiocarcinoma cells by activating the phosphatase shatterproof 2. Hepatology 2009;50:1861-1870.

39. Alemany R, Gomez-Manzano C, Balague C, Yung WK, Curiel DT, Kyritsis AP, Fueyo J. Gene therapy for gliomas: molecular targets, adenoviral vectors, and oncolytic adenoviruses. Exp Cell Res 1999;252:1-12.

40. Curiel DT. Strategies to adapt adenoviral vectors for targeted delivery. Ann N Y Acad Sci 1999;886:158-171.

41. Nagi P, Vickers SM, Davydova J, Adachi Y, Takayama K, Barker S, Krasnykh V, et al. Development of a therapeutic adenoviral vector for cholangiocarcinoma combining tumor-restricted gene expression and infectivity enhancement. J Gastrointest Surg 2003;7:364-371.

42. Saukkonen K, Hemminki A. Tissue-specific promoters for cancer gene therapy. Expert Opin Biol Ther 2004;4:683-696.

43. Lu B, Makhija SK, Nettelbeck DM, Rivera AA, Wang M, Komarova S, Zhou F, et al. Evaluation of tumor-specific promoter activities in melanoma. Gene Ther 2005;12:330-338.

44. Chen JS, Liu JC, Shen L, Rau KM, Kuo HP, Li YM, Shi D, et al. Cancer-specific activation of the survivin promoter and its potential use in gene therapy. Cancer Gene Ther 2004;11:740-747.

45. Ulasov IV, Rivera AA, Sonabend AM, Rivera LB, Wang M, Zhu ZB, Lesniak MS. Comparative evaluation of survivin, midkine and CXCR4 promoters for transcriptional targeting of glioma gene therapy. Cancer Biol Ther 2007;6:679-685.

46. Garg H, Salcedo R, Trinchieri G, Blumenthal R. Improved nonviral cancer suicide gene therapy using survivin promoter-driven mutant Bax. Cancer Gene Ther 2010;17:155-163.

47. Zhu ZB, Makhija SK, Lu B, Wang M, Kaliberova L, Liu B, Rivera AA, et al. Transcriptional targeting of tumors with a novel tumor-specific survivin promoter. Cancer Gene Ther 2004;11:256-262.

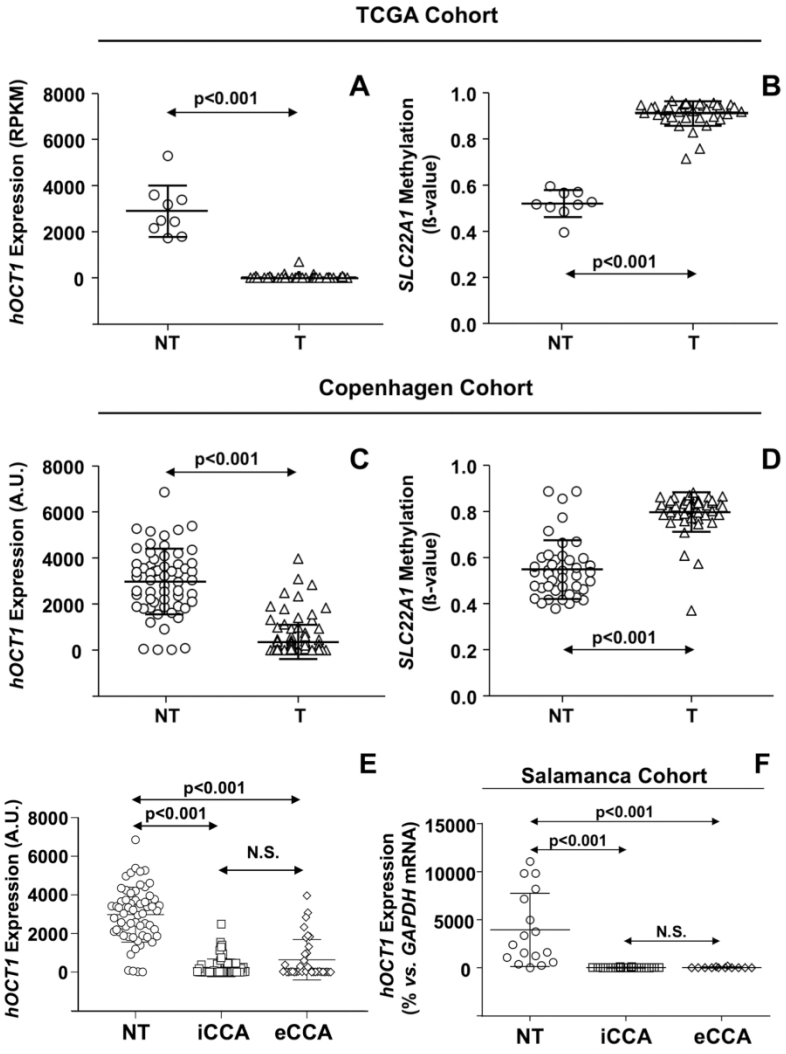

Figure 1

Figure 1

191x276mm (300 x 300 DPI)

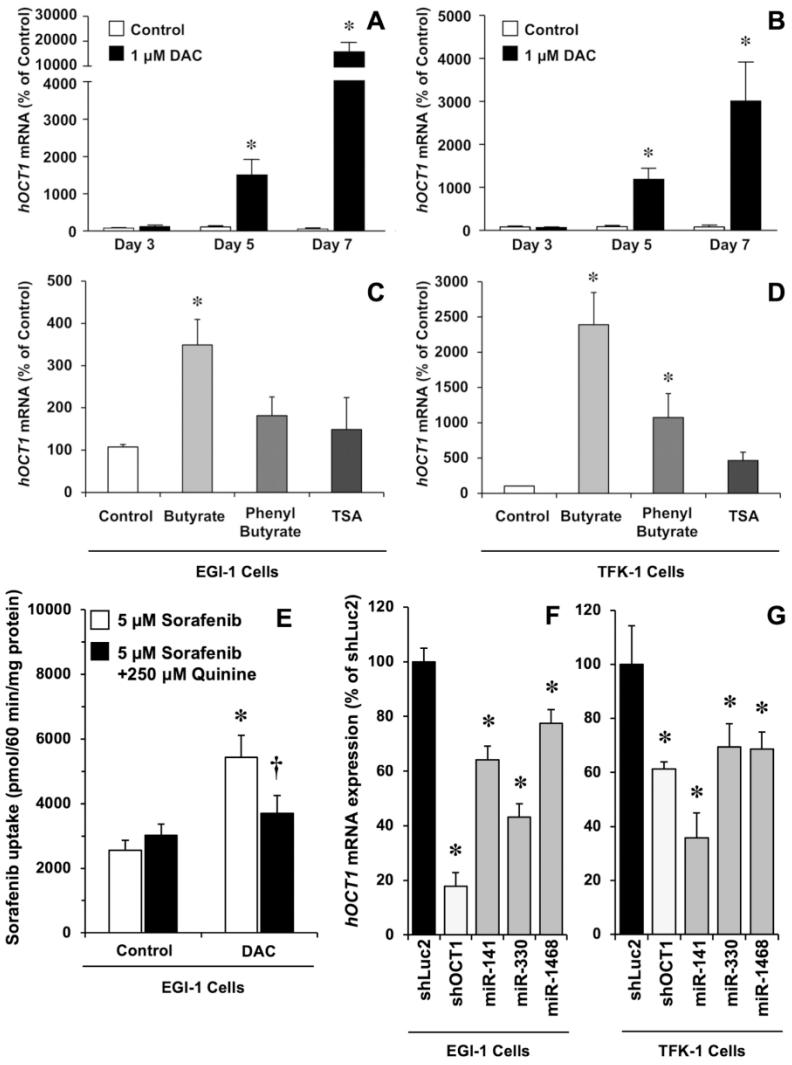

Figure 2

Figure 2

188x265mm (299 x 299 DPI)

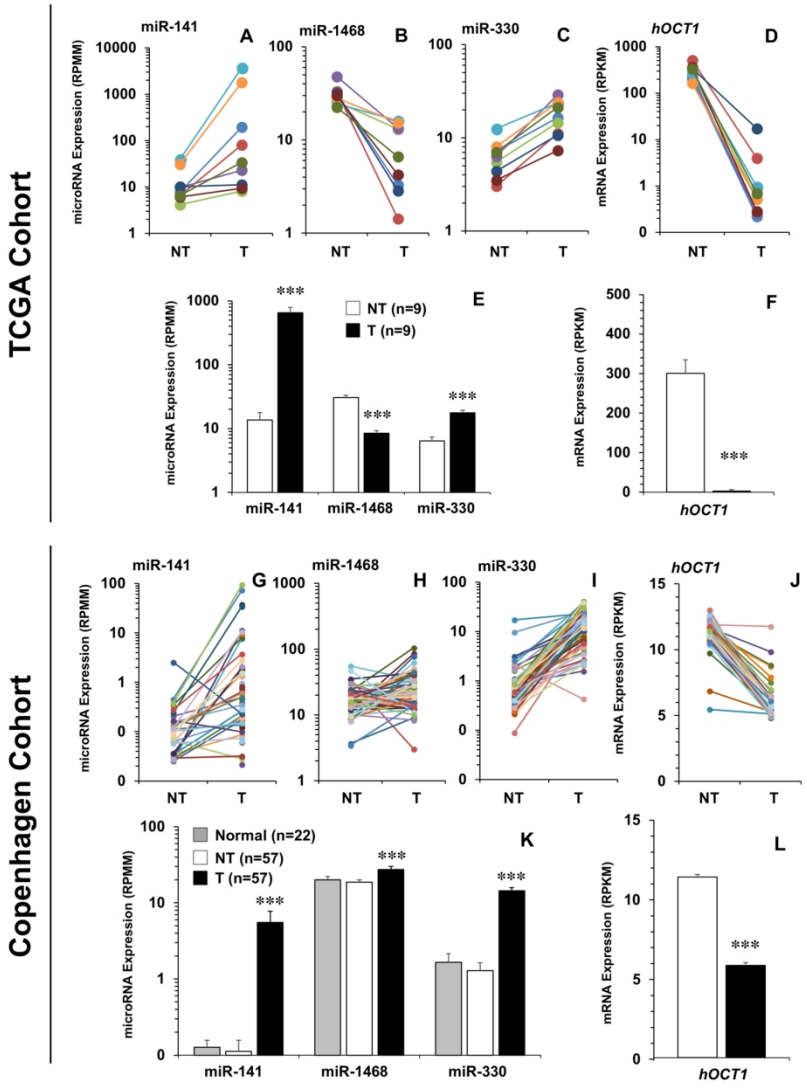

Figure 3

Figure 3

184x258mm (299 x 299 DPI)

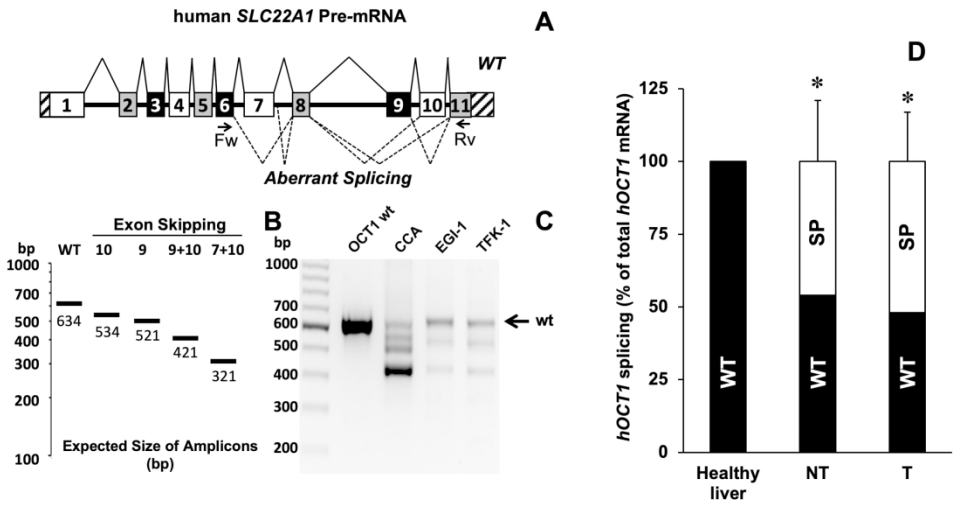

Figure 4

Figure 4

239x156mm (299 x 299 DPI)

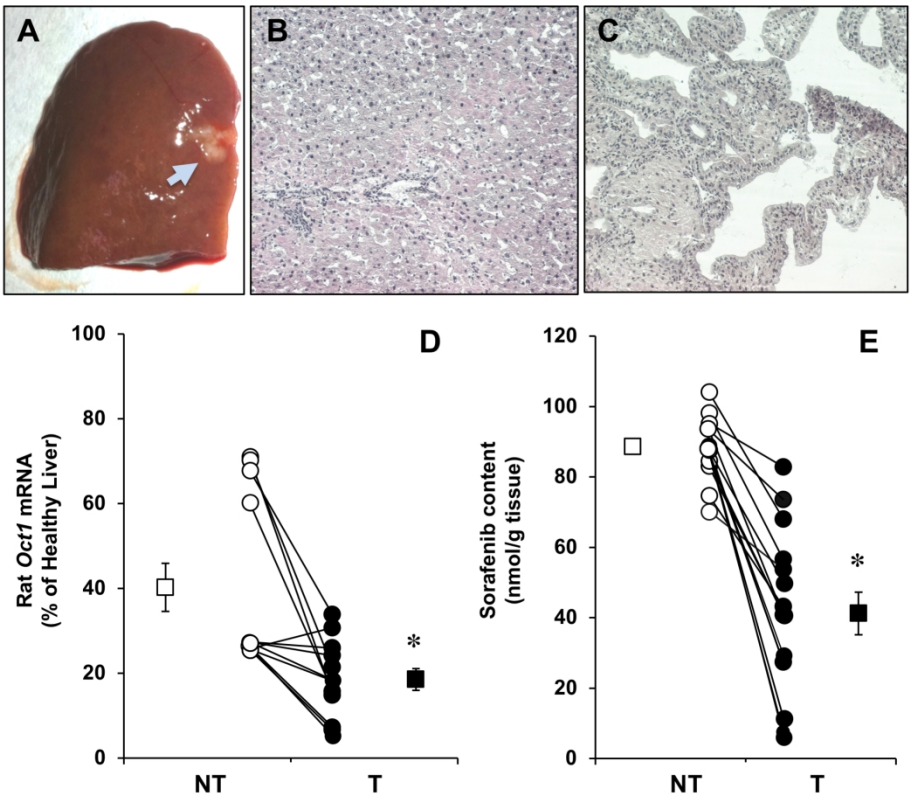

Figure 5

Figure 5

203x183mm (299 x 299 DPI)

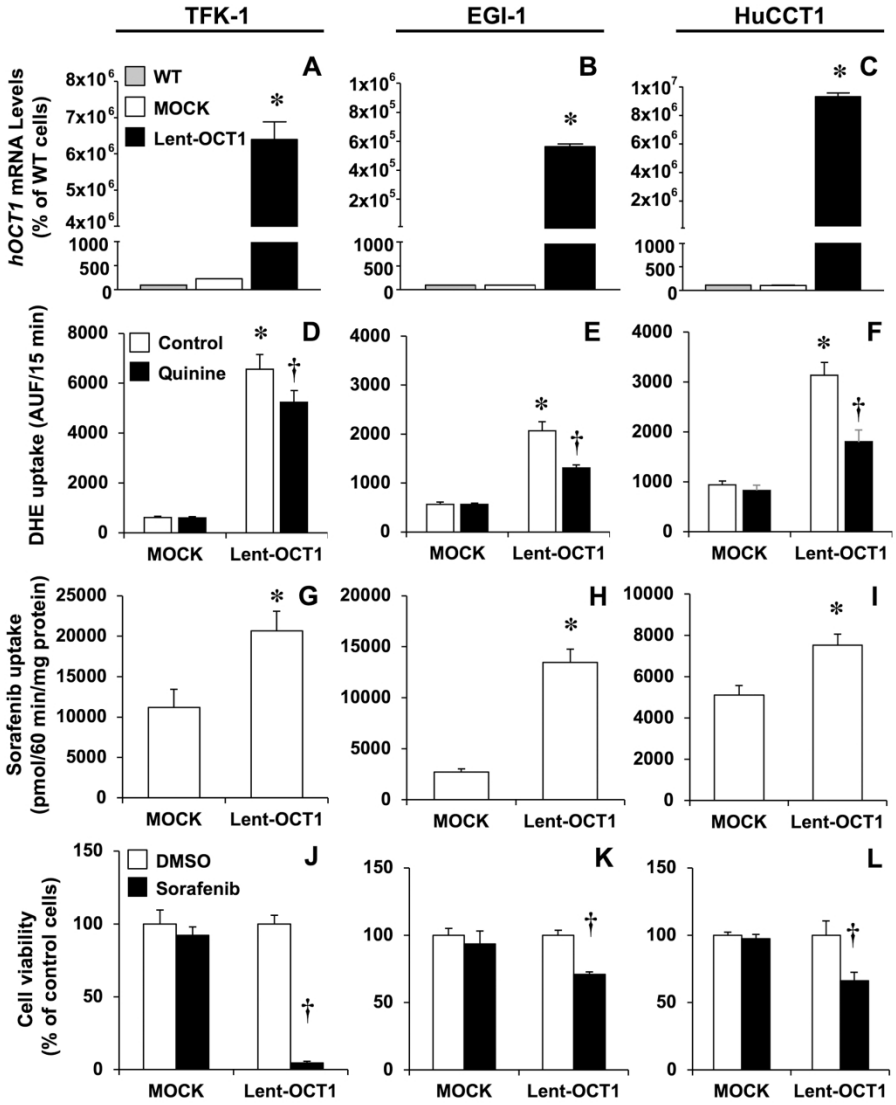

Figure 6

Figure 6

190x254mm (300 x 300 DPI)

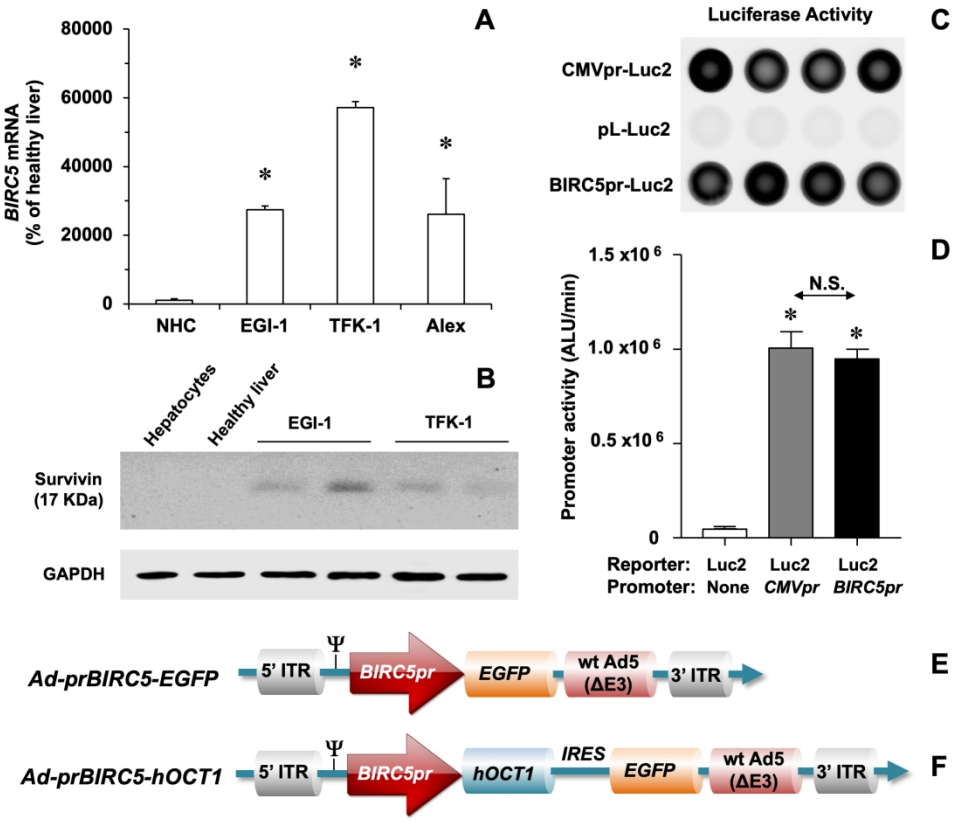

Figure 7

Figure 7

227x213mm (299 x 299 DPI)

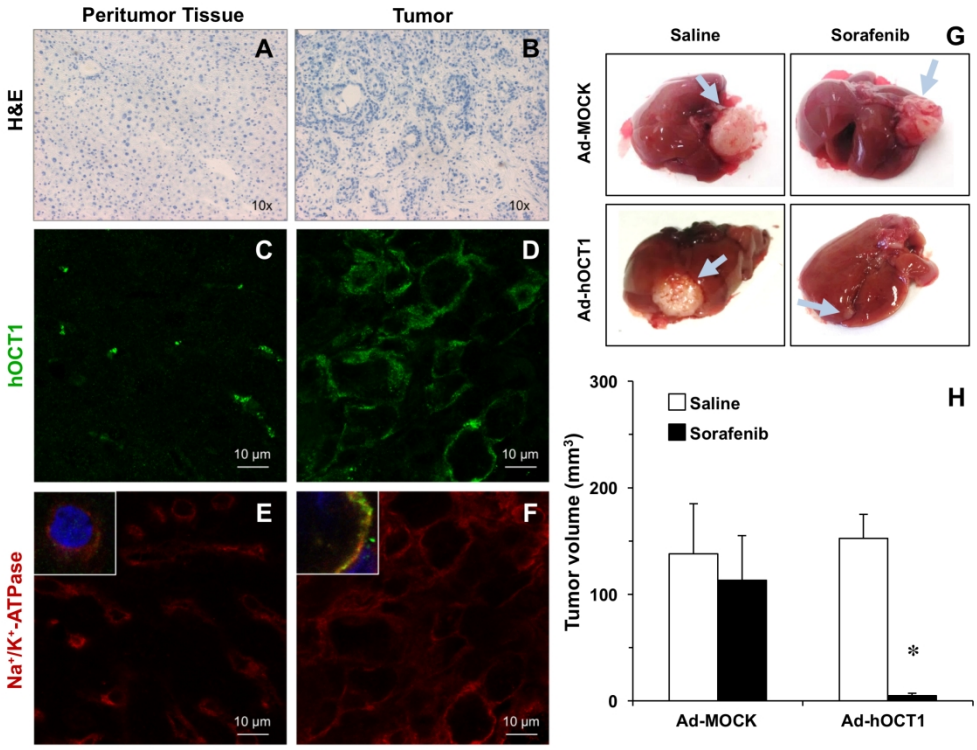

Figure 8

Figure 8

1027x855mm (72 x 72 DPI)

Supporting Information

Material and Methods

Chemicals and Cells. Decitabine (DAC, 5-aza-2'-deoxycytidine), dihydroethidium (DHE), phenyl butyrate, sodium butyrate, trichostatin A (TSA), quinine hydrochloride, and tetraethylammonium (TEA) were obtained from Sigma-Aldrich (Madrid, Spain). Sorafenib was kindly provided by the Pharmacy Department, Salamanca University Hospital (Salamanca, Spain). All other chemicals were of analytical grade.

Human eCCA cells (TFK-1 and EGI-1) were obtained from the German Collection of Microorganisms and Cell Cultures (DSMZ, Braunschwaig, Germany). The human iCCA cell line HuCCT1 was from the Japanese Collection of Research Bioresources (JCRB) Cell Bank (Osaka, Japan). Normal human cholangiocytes (NHC2) (isolated from normal liver tissue) were provided by the Biodonostia Research Institute (1). Alexander or PLC/PRF/5 cells (human HCC) and HEK293T cells (human embryonic kidney, used to generate recombinant lentivirus) were purchased from the American Type Culture Collection. The subclone HEK293A (used to generate recombinant adenovirus) was obtained from Thermo Fisher (Spain). Cells were tested as mycoplasma negative along the experiments.

OCT1 silencing by shRNA or miRNA. The role of miRNAs potentially involved in regulating hOCT1 expression (has-mir-141/330/1468) was studied in EGI-1 and TFK-1 cells, using lentivirus designed to mimic the pre-miRNA sequence including the loop. Commercial DNA oligonucleotides for shRNA targeting hOCT1 (sh-hOCT1; positive control) were obtained from Origene. A shRNA targeted against firefly luciferase (Luc2) was used as a negative control (2). Four oligonucleotides per miRNA were annealed and cloned into the *Mlu*I and *Cla*I restriction sites of the lentiviral pLVTHM plasmid (Supporting Table 5). The selected miRNAs were cloned into the pLVTHM plasmid with the same protocol using oligonucleotides designed to mimic each pre-miRNA sequence including the loop. Lentiviral particles were obtained as described later. These viruses were used to transduce CCA cells that one day after transduction were incubated with 1 μM DAC for 5 days to stimulate basal hOCT1 expression. In all cases eGFP was used as reporter to track transduced cells. The effect on the expression of hOCT1 was investigated using RT-QPCR, carried out as described above, that were obtained 6 days after lentiviral-mediated transduction.

Analysis of hOCT1 Promoter Methylation. The methylation status of hOCT1 promoter was studied using *Infinium HumanMethylation27k BeadChips*. Briefly, DNA was extracted from 48 CCA specimens and 41 paired adjacent non-tumor tissues obtained during surgical resection (subset of Copenhagen cohort). Genomic DNA was isolated using *AllPrep DNA/RNA Universal kit* (Qiagen) and subjected to bisulfite modification with *EZ DNA Methylation-Gold kit* (Zymo Research). Genome-wide DNA methylation profiling was performed as described in the Illumina guidelines and bisulfate-converted DNA-hybridized-chips scanned using *iScan system* (Illumina). Data were analyzed using RnBeads (3) (including Illumina normalization, removal of probes on the X chromosome and those containing 2 or more SNPs). DNA methylation was quantified using beta (β)-value metric (range: 0-1; 0 = 0% methylation, 1 = 100% methylation). Differentially methylated probes (DMPs) were called in cases where mean $\Delta\beta \geq 0.17$ or ≤ -0.17 and Fisher's P-value < 0.05. To further investigate the extent of aberrant DNA methylation in OCT1 promoter, level 1 *Infinium HumanMethylation450 BeadChip* (Illumina Inc.) data were analyzed for 36 CCA tumors through the cancer genome atlas (TCGA). In 9 of these cases, information regarding adjacent non-tumor tissue was available. For 450k data, SNP-enriched probes (≥2 SNPs in 50 base pair probe sequence), X chromosome probes and probes with poor quality, as determined by Greedycut algorithm, were excluded. Data were normalized using beta mixture interquartile (BMIQ) normalization (3) and processed methylation values exported as β-values. Differentially methylated probes (DMPs) and differentially methylated regions (DMRs) were computed using the *RnBeadsintegrated limma* method (hierarchical linear model) followed by model fitting using an empirical Bayes approach.

Analysis of Sorafenib Content in CCA Tumors and Paired Adjacent Tissue in Rats. After 30 weeks of continuous administration of 0.05% thioacetamide (TAA) in the drinking water rats developed CCA (4), and experiments to study sorafenib content in tumor (T) and non-tumor (NT) liver tissue were carried out. The rats were anesthetized with sodium pentobarbital (50 mg/kg b.w., i.p.), a catheter was implanted into the left jugular vein and, after a resting period of 15 min, sorafenib was administered (10 mg/kg b.w., i.v. as a bolus). After 1 h, pieces of T and NT liver tissue were obtained and immediately placed in RNA*later* (Thermo Fisher) or immersed in liquid nitrogen and stored at -80 °C until used for sorafenib content determination by HPLC-MS/MS.

Demethylation and Treatment with HDACIs in CCA Cells. The functional relevance of promoter hypermethylation was evaluated using the demethylating agent DAC. Two CCA cell lines (EGI-1 and TFK-1) were incubated with 1 μM DAC for 3, 5 or 7 days. Fresh medium containing the desired drug concentration was replaced every 24 h. The effect of histone

deacetylase inhibitors (HDACIs), such as sodium butyrate (5 mM), phenyl butyrate (5 mM) and TSA (150 nM) on hOCT1 expression was also evaluated by incubating EGI-1 and TFK-1 cells with each of these HDACIs for 24 h.

Gene Expression Studies: Quantitative RT-PCR. Total RNA extraction from cells or tissues was performed as previously described (5). Retro-transcription was carried out using "SuperScript® VILO™ cDNA Synthesis Kit" (Invitrogen). Real-time quantitative PCR (QPCR) was performed using AmpliTaq Gold polymerase (Applied Biosystems, Madrid) in an ABI Prism 7300 Sequence Detection System (Applied Biosystems) with the following thermal conditions: 1 cycle of 95ºC for 10 min and 40 cycles of 95ºC for 15 s and 60ºC for 60 s. The primer oligonucleotide sequences to carry out QPCR are described in Supporting Table 3. The results of mRNA abundance for target genes in each sample were normalized on the basis of human *GAPDH*, *HPRT1* or rat *β-actin* mRNA abundance. Detection of amplification products was carried out using SYBR Green I. Total RNA from control liver was used as a calibrator. Expression levels were calculated as $2^{-\Delta\Delta Ct}$, where ΔCt was the difference of Ct in each sample between the target gene and the normalizer. This was used to calculate $\Delta\Delta Ct$ as the difference of this value between control RNA and experimental groups.

Recombinant Lentiviruses Production and Lentiviral-Mediated Transduction. Recombinant lentiviruses were produced in HEK293T cells transfected using a standard polyethylenimine (PEI) protocol with the transfer vector pWPI-hOCT1, encoding both hOCT1 and EGFP or simply pWPI (to generate "empty vectors"), and the packaging plasmids psPAX2 and pMD2.G. Viral titers were determined by transduction of HEK293T cells with serial dilutions of the viral suspension, and determination of the percentage of EGFP-positive cells by flow cytometry (FACSCalibur, BD Biosciences, Madrid). Lentiviral vectors were added to target cells at a multiplicity of infection (MOI) of 25 infectious particles per cell in the presence of polybrene. The cells were incubated for 4 days prior to be used.

Cloning Procedures and Vector Constructions to Generate Adenoviral Vectors. A 1467-bp zone of the 5′-flanking region of the *BIRC5* gene, considered as the promoter region (*BIRC5pr*), was cloned using genomic DNA obtained from Alexander HCC derived cells. The construct was amplified by PCR using the high fidelity AccuPrime Pfx DNA polymerase (Invitrogen), and specific oligonucleotide primers (Supporting Table 2) to which *attB* sites were added to obtain cDNA adapted for Gateway cloning. PCR products were recombined with the pDONR221 vector (Invitrogen) to generate an Entry plasmid, which was further recombined with the pcDNA-6.2 destination vector (Invitrogen) and with another Entry plasmid that contained the coding sequence of hOCT1. This was cloned as we previously

described (6) and was recombined with the pDONOR221 vector to generate this ENTRY plasmid. The destination vector encoding BIRC5pr-hOCT1 was modified by PCR to add suitable *attL1* and *attR5* sites to carry out the LR reaction with an Entry plasmid encoding IRES-EGFP and the pAd/PL-DEST (ViraPower Adenoviral Expression System, Invitrogen; that contain elements of human adenovirus type 5). The resultant plasmid was purified, and its sequence was confirmed. Then it was digested with *Pac*I, to expose the ITRs, and transfected into the HEK293A producer cell line that supplies the E1a and E1b proteins necessary to generate adenovirus, following the supplier instructions. Once a crude stock of adenovirus was obtained, this was amplified by infection of HEK293A. Adenovirus were purified using ViraBind™ Adenovirus Miniprep kit (Cell Biolabs) and then viral titers were determined by transduction of EGI-1 cells with serial dilutions of the viral solution and analysis of EGFP-positive cells with a FACSCalibur flow cytometer, or by the quantification of EGFP expression in the viral solution by quantitative PCR. A similar process was followed to generate control adenoviruses (Ad-Mock) that contain *BIRC5pr* and IRES-EGFP (see Fig. 7E and 7F).

BIRC5 vs CMV Promoter-Reporter Assays. Plasmids containing firefly luciferase (Luc2) fused to *BIRC5pr* or *CMVpr* were design in order to carry out promoter reporter assays by cell transient transfection. *BIRC5pr* with the appropriated *attB* sites adapted for Gateway cloning was recombined with the pDONR221 vector (Invitrogen) to generate an Entry plasmid, which was further recombined with the pcDNA-6.2-pL destination vector (Invitrogen) and with another Entry plasmid that contains the coding sequence of Luc2. This plasmid was generated using as template the pGL4.10[Luc2] plasmid (Promega, Madrid, Spain) to amplify the coding sequence of Luc2 using specific primers with the appropriated adapters (6). Promoter reporter assays were carried out by transient transfection with BIRC5pr-Luc2 or CMVpr-Luc2 plasmids and promoterless “pL-Luc2” as negative control. These experiments were carried out using human hepatoma Alexander cells due to the high efficiency in transfection reached with these cells. Briefly, Alexander cells were seeded at subconfluence (≈5000 cells/w) in 96 well/plates and the following day they were transiently transfected using Lipofectamine LTX/PLUS reagent (Life Technologies). 48 h after transfection luciferase activity was evaluated by measuring light generation in the presence of the substrate luciferine using the Bright-Glo Luciferase Assay System (Promega) in a LAS-4000 image reader (FujiFilm; TDI, Madrid, Spain). The results were expressed as arbitrary light units/min.

DHE, TEA and Sorafenib Transport Assays. Cells transduced with lentivirus or after DAC treatment were seeded at subconfluence (≈75,000 cells/well) in 24 well plates and the experiments were performed the day after. To carry out uptake experiments using TEA (a

typical substrate of OCT1) the cells were incubated with medium containing 150 µM [^{14}C]-TEA (PerkinElmer, Barcelona, Spain) without or with 250 µM quinine for 60 min at 37 ºC. Uptake experiments using DHE, other cationic compound substrate of OCT1, were performed by incubation of the cells with medium containing 5 µM DHE without or with 250 µM quinine at 37ºC for 15 min. Then, intracellular fluorescence was determined by flow cytometry. For sorafenib uptake experiments the medium contained 5 µM sorafenib and the cells were incubated for 60 min. Uptake was stopped by rinsing the cells 4 times with 1 ml of ice-cold medium. Cells were then lysed using pure water. Sorafenib concentrations in the lysates were determined using an adaptation of a previously published method to determine its content by high-performance liquid chromatography-dual mass spectrometry (HPLC-MS/MS) (7). The results were corrected by protein content (8).

Immunofluorescence and Immunoblotting Assays. Immunofluorescent staining was performed on tissue cryosections air-dried and fixed in cold methanol using antibodies against hOCT1 (LS-C161155, LifeSpan BioSciences), CD31 (PECAM1 clone MEC 13.3, BD Pharmigen) and Na^+/K^+-ATPase (ab2871, Abcam) diluted 1:50, 1:50 and 1:100, respectively, in 2% fetal calf serum in phosphate-buffered saline (PBS). Alexa Fluor-594 anti-rat and cyanin-5-conjugated anti-rabbit IgG secondary antibodies were diluted 1:1000 and 1:500, respectively (Molecular Probes, Leiden, The Netherlands). Nuclei were counterstained with DAPI. Confocal laser-scanning microscopy was performed using a Leica TCS SP2 confocal microscope.

To carry out western-blot analyses, cell lysates (30 µg/lane) were separated by 10% SDS-PAGE. Primary antibodies for p-STAT3 (9145s, Cell Signaling), STAT3 (ab7966, Abcam) or GAPDH (sc-32233, Santa Cruz Biotechnology) were diluted 1:1000 in 5% w/v BSA, 1X TBS, 0.1% Tween. Immunoreactive protein bands were visualized by ECL (Amersham Pharmacia Biotech) after incubation with appropriate secondary antibodies (IgG-HRP linked).

References

1. Banales JM, Saez E, Uriz M, Sarvide S, Urribarri AD, Splinter P, Tietz Bogert PS, et al. Up-regulation of microRNA 506 leads to decreased Cl-/HCO3- anion exchanger 2 expression in biliary epithelium of patients with primary biliary cirrhosis. Hepatology 2012;56:687-697.
2. Gonzalez-Sanchez E, Perez MJ, Nytofte NS, Briz O, Monte MJ, Lozano E, Serrano MA, et al. Protective role of biliverdin against bile acid-induced oxidative stress in liver cells. Free Radic Biol Med 2016;97:466-477.
3. Assenov Y, Muller F, Lutsik P, Walter J, Lengauer T, Bock C. Comprehensive analysis of DNA methylation data with RnBeads. Nat Methods 2014;11:1138-1140.
4. Lozano E, Sanchez-Vicente L, Monte MJ, Herraez E, Briz O, Banales JM, Marin JJ, et al. Cocarcinogenic effects of intrahepatic bile acid accumulation in cholangiocarcinoma development. Mol Cancer Res 2014;12:91-100.
5. Martinez-Becerra P, Vaquero J, Romero MR, Lozano E, Anadon C, Macias RI, Serrano MA, et al. No correlation between the expression of FXR and genes involved in multidrug resistance phenotype of primary liver tumors. Mol Pharm 2012;9:1693-1704.
6. Herraez E, Gonzalez-Sanchez E, Vaquero J, Romero MR, Serrano MA, Marin JJ, Briz O. Cisplatin-induced chemoresistance in colon cancer cells involves FXR-dependent and FXR-independent up-regulation of ABC proteins. Mol Pharm 2012;9:2565-2576.
7. Herraez E, Lozano E, Macias RI, Vaquero J, Bujanda L, Banales JM, Marin JJ, et al. Expression of SLC22A1 variants may affect the response of hepatocellular carcinoma and cholangiocarcinoma to sorafenib. Hepatology 2013;58:1065-1073.
8. Markwell MA, Haas SM, Bieber LL, Tolbert NE. A modification of the Lowry procedure to simplify protein determination in membrane and lipoprotein samples. Anal Biochem 1978;87:206-210.

Legend to Supporting Figures

Supporting Figure 1. Hypermethylation of SLC22A1 gene. Methylation levels from TCGA cohort of SLC22A1 promoter in CCA tumors (T; n=36) compared to paired non-tumor (NT; n=9) tissue (mean±SD; p-value *vs.* controls was p<0.0001, Mann-Whitney t-test) using three probes: (A) cg13434757 (TSS1500 of SLC22A1); (B) cg13466809 (5'UTR/exon 1 of SLC22A1), and (C) cg24864413 (TSS200 of SLC22A1).

Supporting Figure 2. Changes in mRNA expression of genes related with RNA stability/decay. Relative mRNA levels of HuR (A), AUF1 (B), BRF1 (C), BRF2 (D), CUGBP (E), FBP2 (F) and TTP (G), in human CCA (T, n=9) and adjacent non-tumor (NT, n=8) tissue. Gene names and their effect on mRNA stability or decay (H). Results are shown as individual values (circles) and as mean±SD (squares). *, p<0.05 comparing T with NT; N.S. = not significant, p>0.05.

Supporting Fig. 3. Tetraethylammonium uptake by CCA cells overexpressing OCT1. TFK-1 and EGI-1 cells transduced with control lentivirus (MOCK) or hOCT1 lentivirus (Lent-OCT1) were incubated with 150 μM [^{14}C]-TEA in the absence (Control) or the presence of 250 μM quinine for 1 h to determine hOCT1 function. Values are mean±SD from three experiments performed in triplicate. *, p<0.05, as compared to MOCK groups. †, p<0.05, on comparing to cells incubated in absence of quinine.

Supporting Figure 4. Sorafenib-induced inhibition of STAT3 phosphorylation. Immunoblotting analyses of pSTAT3, STAT3 and GAPDH in TFK1 cells transduced with lentiviral vectors either empty (MOCK or hOCT1 -) or containing hOCT1 ORF (hOCT1 +). Cells were incubated without or with 5 μM sorafenib for 4 h and then cultured in sorafenib-free medium for an additional 20-h period. Cells were then collected to obtain the lysates and proteins (30 μg/lane) were separated by 10% SDS-PAGE.

Supporting Figure 5. Absence of hOCT1 expression in endothelial cells. PECAM-1 and hOCT1 were detected by immunofluorescence in tumors generated by implanting EGI-1 tumor fragments (≈1 mm^3) in the liver of nude mice. Adenoviral vector Ad-prBIRC5-hOCT1 was administered (i.v.) every 5 days for 2 months to induce hOCT1 expression. Immunofluorescence localization of PECAM-1 and hOCT1 in tumor cryosections was carried out by staining with anti-PECAM-1 (red) and anti-OCT1 (green). Nuclei were stained with Dapi (blue). Cy5 fluorescence was artificially converted into green.

Supporting Figure 6. Effect of sorafenib treatment on vascular density. Representative images of immunofluorescence localization of PECAM-1 in tumors generated by implanting EGI-1 tumor fragments (≈1 mm^3) in the liver of nude mice. Adenoviral vector Ad-prBIRC5-hOCT1 was administered (i.v.) every 5 days for 2 months to induce hOCT1 expression. Mice were treated with saline (Control) or sorafenib (10 mg/kg b.w, i.p.) twice per week. Cryosections were stained with anti-PECAM1 (red) antibody (A, B). Nuclei were stained with Dapi (blue). Red image was extracted and digitized (C-J) to then measure the proportion of stained area (K). *, $p<0.05$ on comparing Control (n=5) and sorafenib (n=5) groups.

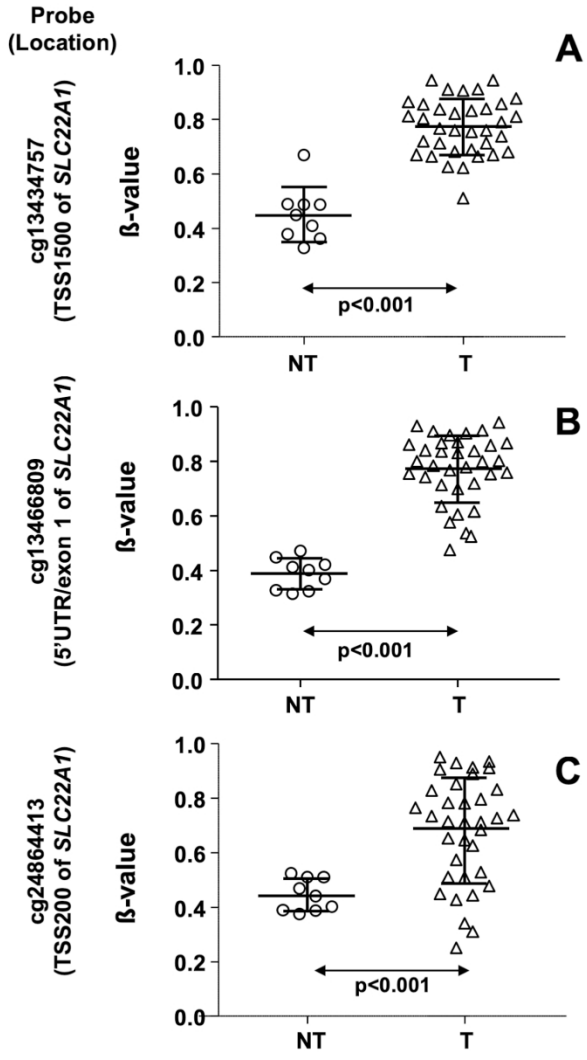

Supporting Figure 1

127x223mm (299 x 299 DPI)

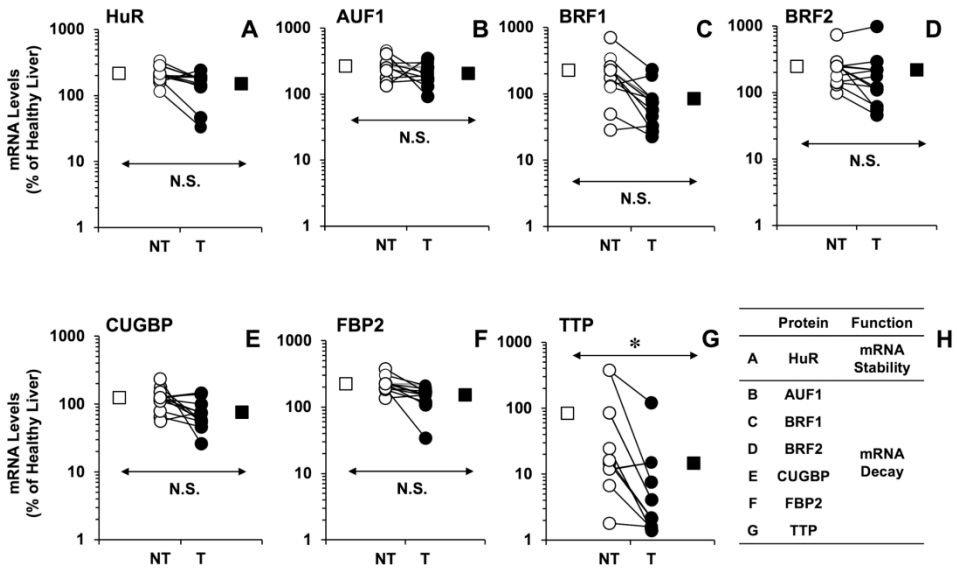

Supporting Figure 2

264x174mm (299 x 299 DPI)

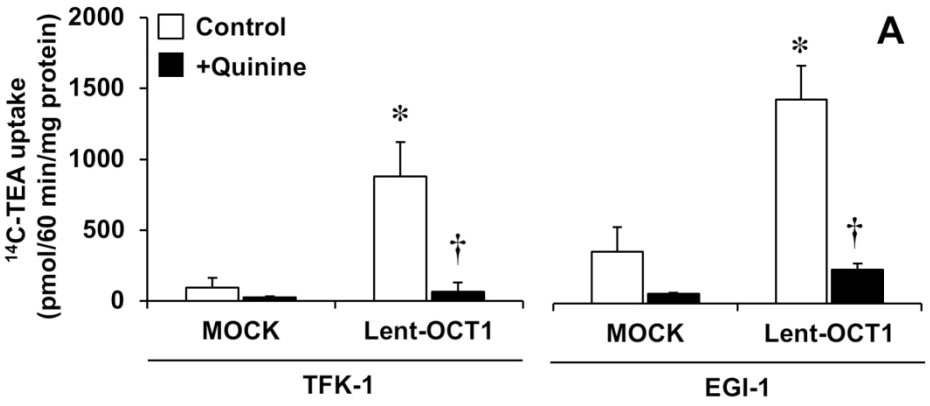

Supporting Figure 3

165x88mm (299 x 299 DPI)

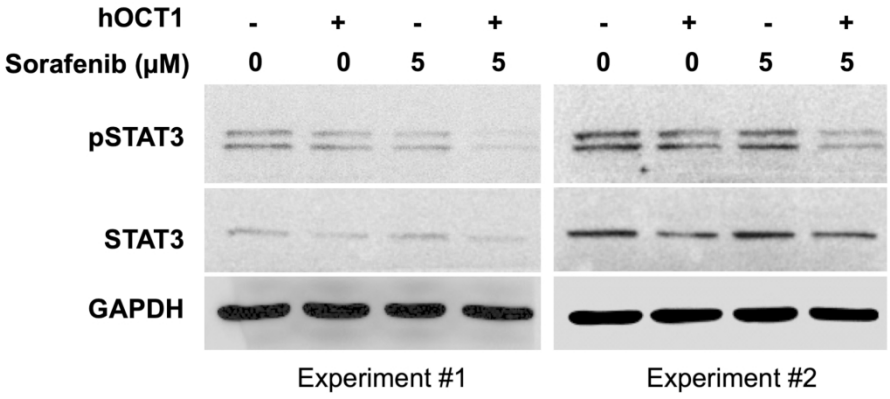

Supporting Figure 4

185x120mm (299 x 299 DPI)

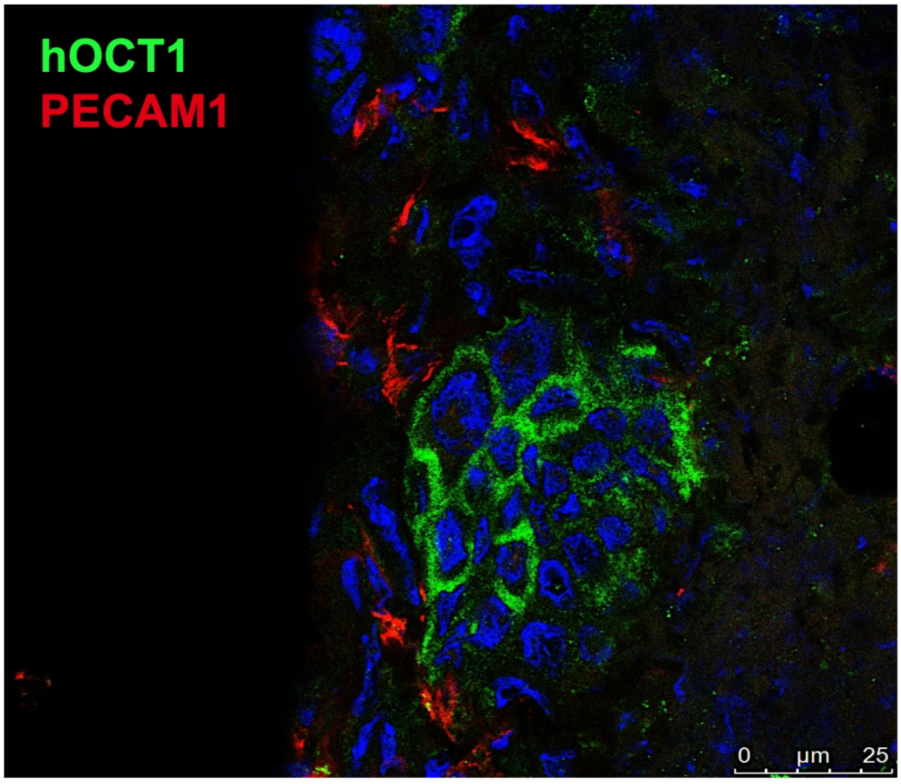

Supporting Figure 5

153x142mm (299 x 299 DPI)

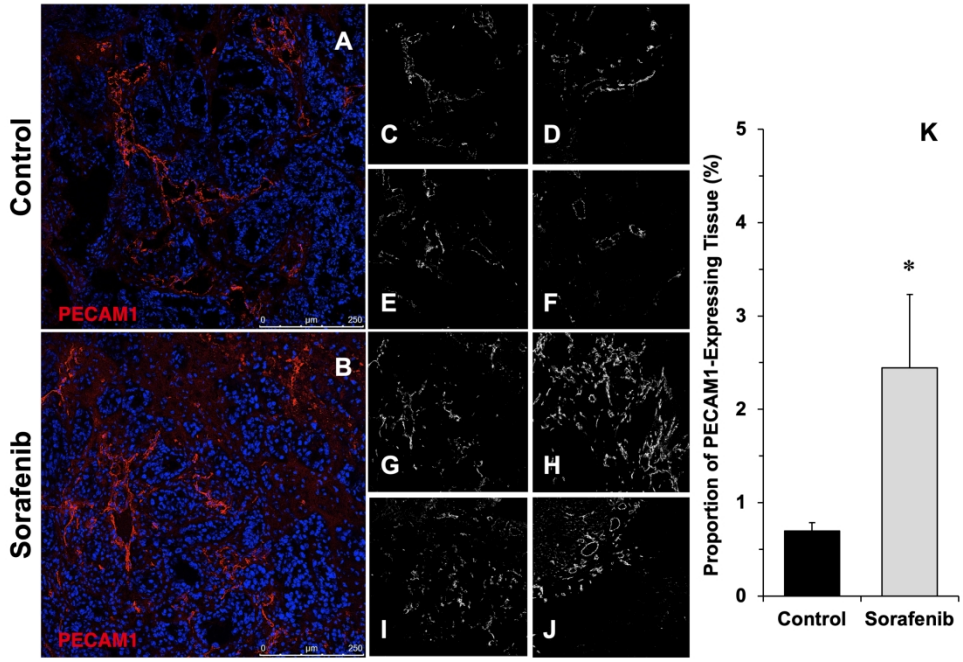

Supporting Figure 6

254x191mm (299 x 299 DPI)

Supporting Table 1. Characteristics of patients and tumors included in the "Salamanca cohort".

Patient ID	Age	Gender	Type of Tumor	Tumor Stage
1	52	M	iCCA	II
2	76	F	iCCA	IVA
3	65	F	iCCA	II
4	58	M	iCCA	I
5	75	M	iCCA	NA
6	50	F	iCCA	NA
7	56	F	pCCA	II
8	81	F	iCCA	II
9	83	F	iCCA	II
10	50	M	iCCA	II
11	48	F	pCCA	II
12	62	M	iCCA	II
13	72	M	pCCA	IV
14	79	M	dCCA	II
15	75	F	dCCA	II
16	70	F	iCCA	I
17	80	F	dCCA	II
18	82	M	dCCA	II
19	65	M	dCCA	I
20	72	M	dCCA	II
21	71	M	iCCA	II
22	71	M	iCCA	I
23	73	M	dCCA	II
24	63	M	iCCA	NA
25	64	M	iCCA	II
26	69	M	iCCA	I
27	71	M	pCCA	NA
28	71	M	pCCA	NA

The Salamanca cohort includes intrahepatic (iCCA) and extrahepatic (eCCA) cholangiocarcinomas. The eCCA group includes distal (dCCA) and perihilar (pCCA) cholangiocarcinomas; ID, identification; F, female; M, male; NA, not available.

Supporting Table 2. Oligonucleotide sequence of specific primers for the cloning of *hOCT1* coding sequence and *BIRC5pr* used in this study.

Application	Sequence (5'-3')	Type
***hOCT1 ORF* Amplification**	ATGCCCACCGTGGA	F
	GGTGCCCGAGGGTTCTG	R
Sequencing *hOCT1 mRNA*	GCCCGAGGGTTCTGAGGTTT	R
	GAAGGGCTCAGCTTTTCGGTGA	R
	GGTGGCTGTTATCACAAAAAAGAAACACTGAA	F
	CAGGTGCCCGAGGGTTCT	R
	GGCTCCAGCCACAGCG	R
***BIRC5pr* Amplification**	AAATTGACATCGGGCCGGG	F
	GCCGCCGCC	R
IRES-EGFP Amplification	GGGCTGCAGGAATTCCGC	F
	CTAGCTACTAGCTAGTCGAGATCTGAGTCC	R
Sequencing *BIRC5pr*	GGGCGATAGAGCGAGACTCAGT	F
	GGTGTGCCGGGAGTTGTAGT	R

Forward (F) and reverse (R) primers used to amplify the hOCT1 ORF included a *Pac*I restriction site for cloning into the pWPI plasmid, and the forward primer also contained the Kozak consensus sequence for optimal expression.

Supporting Table 3. Sequence of oligonucleotide primers used for quantitative PCR.

Gene	Accesion number	Forward primer (5' – 3')	Reverse primer (5' – 3')
hOCT1	NM_003057	TGCAGACAGGTTTGGCCGT	GCCCGAGCCAACAAATTCTGTGAT
hOCT1 Spliced	NM_003057	GGAAGCGCACCTTCATCCTGAT	CAGGTGCCCGAGGGTTCT
hAUF1	NM_001003810	GTAAGAACGAGGAGGATGAAGGGAAAATGT	TTGATCCATGACCTTATCTACACTCTCCGA
hBIRC5	NM_001168	CCAGATGACGACCCCATAGAGGAA	GCACTTTCTCCGCAGTTTCCTCA
hCUGBP	NM_006560	CCTCAGAGCAAAGGGTGCTGTT	TCCTGTCTTCCACTGCATTGTTCTTCT
hHUR	NM_001419	CGGGATAAAGTAGCAGGACACAGCTT	GGGCGAGCATACGACACCTT
hTTP	NM_003407	CTGCCATCTACGAGAGCCTCCT	GCGAAGTGGGTGAGGGTGA
hBRF1	NM_004926	GCGTGTGGGACTCCAGACA	TCTTGTTACCCTTGCATAAAACTTCGCTCA
hBRF2	NM_006887	CCCGTTATTCGTCGTGGCTCAA	CCAGGGATTTCTCTGTCTTGCACA
hFBP2	NM_003685	GTTGGAAGATGGAGATCAACCGGAGA	GTCATTGAAGTCCTTGGGGGAGGAT
hGAPDH	NM_002046	TGAGCCCGCAGCCTCC	TACGACCAAATCCGTTGACTCC
hHPRT1	NM_000194	GCCCTGGCGTCGTGATTAGT	AGCAAGACGTTCAGTCCTGTCCATAA
ratOCT1	NM_012697	CATTGCAGACAGGTTTGGCCGTAA	GCAGGCGAAAGAGCAACATGGAT
ratACTB	NM_031144	TCTGTGTGGATTGGTGGCTCTA	CTGCTTGCTGATCCACATCTG

Supporting Table 4. Biochemical markers of liver and kidney function in mouse plasma

	Protein g/dl	Albumin g/dl	Bilirubin mg/dl	AST IU/l	ALT IU/l	BUN mg/dl	Uric acid mg/dl	Creatinine mg/dl	n
Control	3.7±0.1	1.9±0.1	0.4±0.1	86±52	16±9	25±4	1.3±0.1	0.5±0.1	5
AD-MOCK	3.7±0.3	1.9±0.1	0.4±0.1	79±47	12±4	20±1	1.4±0.7	0.4±0.1	3
AD-MOCK+Sorafenib	4.1±0.2	2.0±0.3	0.4±0.1	82±52	10±1	23±1	1.2±0.4	0.4±0.1	4
AD-OCT1	3.0±0.9	1.9±0.1	0.3±0.1	51±8	11±2	22±4	1.6±0.6	0.4±0.1	3
AD-OCT1+Sorafenib	4.0±0.7	1.9±0.1	0.4±0.1	57±25	10±1	22±3	1.5±0.5	0.6±0.1	4

Mice receiving the vehicle (saline) alone (Control) were used for comparative purposes. Values are expressed as mean±SD. AST, aspartate aminotransferase; ALT, alanine aminotransferase; BUN, blood urea nitrogen. No significant differences ($p>0.05$) were observed among groups by the Bonferroni method of multiple range testing.

Supporting Table 5. Sequence of forward (F) and reverse (R) oligonucleotide primers used for cloning of shOCT1, shLuc2 or the selected miRNAs.

Gene		Oligonucleotide sequence 5' – 3'
sh-OCT1	F	CGCGTAAGAACGGTGGCGATCATGTACCAGATGGTTCAAGAGACCATCTGGTACATGATCGCCACCGTTCTTTTTTTGGAAAT
	R	CGATTTCCAAAAAAAGAACGGTGGCGATCATGTACCAGATGGTCTCTTGAACCATCTGGTACATGATCGCCACCGTTCTTA
sh-Luc2	F	CGCGTCTGACGCGGAATACTTCGATTCAAGAGATCGAAGTATTCCGCGTCAGTTTTTGGAAATCG
	R	CGATTTCCAAAAACTGACGCGGAATACTTCGATCTCTTGAATCGAAGTATTCCGCGTCAGACGCG
hsa-mir-330	F1	CGCGTCTTTGGCGATCACTGCCTCTCTGGGCCTGTGTCTTAGGCTCTGCAAGA
	R1	GGTTGATCTTGCAGAGCCTAAGACACAGGCCCAGAGAGGCAGTGATCGCCAAAGA
	F2	TCAACCGAGCAAAGCACACGGCCTGCAGAGAGGCAGCGCTCTGCCCAT
	R2	CGATGGGCAGAGCGCTGCCTCTCTGCAGGCCGTGTGCTTTGCTC
hsa-mir-141	F1	CGCGTCGGCCGGCCCTGGGTCCATCTTCCAGTACAGTGTTGGATGGTCTAAT
	R1	GCTTCACAATTAGACCATCCAACACTGTACTGGAAGATGGACCCAGGGCCGGCCGA
	F2	TGTGAAGCTCCTAACACTGTCTGGTAAAGATGGCTCCCGGGTGGGTTCTTTTTGGAAAT
	R2	CGATTTCCAAAAAGAACCCACCCGGGAGCCATCTTTACCAGACAGTGTTAGGA
hsa-mir-1468	F1	CGCGTGGTGGGTGGTTTCTCCGTTTGCCTGTTTCGCTGATGTGCATTC
	R1	AGTTGAATGCACATCAGCGAAACAGGCAAACGGAGAAACCACCCACCA
	F2	AACTCATTCTCAGCAAAATAAGCAAATGGAAAATTCGTCCATCTTTTTGGAAAT
	R2	CGATTTCCAAAAAGATGGACGAATTTTCCATTTGCTTATTTTGCTGAGAATG